

Master's Programme in Chemical and Metallurgical Engineering

Investigating the Influence of forced-air Pneumatic Flotation Cell on the Recovery of Fine Pentlandite

Lassi Pekkanen

Master's thesis
2025

Copyright ©2025 Lassi Pekkanen

Author	Lassi Pekkanen	
Title of thesis	Investigating the influence of forced-air pneumatic flotation cell on the recovery of fine pentlandite	
Programme	Chemical and Metallurgical engineering	
Major	Sustainable Metallurgical Engineering.	
Thesis supervisor	Prof. Rodrigo Serna	
Thesis advisor(s)	Dr. Benjamin Musuku, D.Sc. (Tech)	
Collaborative partner	Boliden Kevitsa Mining	
Date	Number of pages	Language
6.10.2025	57+11	English

Abstract

Due to depleting ore reserves around the world, extraction of more complex ore-bodies has become more common. This has led to the need for finer grinding in order to liberate the valuable minerals from the gangue minerals. Traditional flotation cells are not able to recover particles under 25 microns efficiently and thus need for new flotation technologies for fine particle floatation has emerged. Metso's Concorde Cell™ is a forced-air pneumatic flotation cell which operates at high shear rates, high circulating load and with fine disseminated bubbles to enhance recovery of fine particles. In January 2025 Concorde Cell™ was commissioned at Boliden Kevitsa mill with the goal to improve recovery of nickel. This thesis focused on studying the effects of Concorde Cell™ on the recovery of total and fine nickel particles. Paired sampling campaigns, with and without Concorde, were conducted for four days to observe Concorde Cell™ performance with two different feed streams namely rougher concentrates and cleaner three tails. Due to the small size of the Concorde cell™, effects on the circuit were not significant. Varying feed grades impacted the final recoveries of the circuit. Plant performance improved slightly with one of the feeds to the Concorde Cell™. Concorde Cell™ itself was able to produce high-grade concentrates.

Keywords Flotation, Flotation circuit, Nickel, Pentlandite, Fine particle flotation, Concorde Cell™

Tekijä Lassi Pekkanen

Työn nimi Pneumaattisen vaahdotuskennon vaikutus hienojakoisen pentlandiitin talteenottoon.

Koulutusohjelma Chemical and Metallurgical Engineering.

Pääaine Sustainable Metallurgical Engineering.

Vastuuopettaja/valvoja Prof. Rodrigo Serna

Työn ohjaaja(t) TkT Benjamin Musuku

Yhteistyötaho Boliden Kevitsa Mining

Päivämäärä 6.10.2025 **Sivumäärä** 57+11 **Kieli** Englanti

Tiivistelmä

Heikentyneiden malmivarantojen takia monimutkaisimpien malmioiden hyödyntäminen on yleistynyt viime vuosina. Tämän takia malmia on jauhettava entistä hienommaksi, jotta arvokkaat mineraalit erottuvat muista mineraaleista. Yleiset vaahdotuskennot talteen ottavat heikosti alle 25 mikronin kokoisia partikkeleita, jonka takia viime vuosina uusia vaahdotusteknologioita pienten partikkeleiden talteen ottamiseksi on kehitetty. Metson Concorde Cell™ on paineilmalla toimiva pneumaattinen vaahdotuskenno, joka toimii korkealla paikallisenergialla, korkealla kiertokuormalla, sekä käyttää hienoja kuplia pienten partikkelien tehokkaampaan talteenottoon. Tammikuussa 2025 Bolidenin Kevitsan rikastamolla otettiin käyttöön yksi Concorde Cell™ vaahdotuskenno, tavoitteena parantaa nikkelin saantia. Tässä diplomityössä keskityttiin tutkimaan Concorde Cell™ vaahdotuskennon vaikutuksia nikkelin saantiin, sekä hienojakoisen nikkelin saantiin Bolidenin Kevitsan nikkelivaahdotuspiirissä. Neljän päivän aikana suoritettiin näytekampanja, jolla selvitettiin vaahdotuspiirin tehokkuus ennen kennon asennusta, sekä kennon vaikutukset kahdella eri syötteellä. Kennon pienen koon takia vaikutukset eivät olleet huomattavia. Vaihtelevat syötepitoisuudet vaikuttivat lopullisiin saanteihin. Vaahdotuspiirin tehokkuus parani hieman toisella syötteellä Concorde Cell™ kanssa. Concorde Cell™ pystyi itsessään tuottamaan korkeapitoista nikkeli-rikastetta.

Avainsanat Vaahdotus, vaahdotuspiiri, Nikkeli, Pentlandiitti, hienovaahdotus, Concorde Cell™

Acknowledgements

When I started my studies, I had no idea what I would want to study or where I would end up in. Luckily, in the early stages of my studies I found Vuorimieskilta. Through Vuorimieskilta I got to visit different mines and factories which made me realize that mining is where I want to end up in. I would like to express my gratitude to Vuorimieskilta for the countless happy memories during my studies and many new friends I got to meet and who helped me forward in my studies.

I am especially appreciative of Boliden Kevitsa Mining Oy for the opportunity to make this thesis in Kevitsa and for the many summers I have had the chance to work at the mine. Thanks to all the great people at the Kevitsa mill, especially shift workers, for warmly welcoming me to Lapland and teaching me a lot about mining and minerals processing. I am sure that all these skills will help me a lot during my future career.

Thank you to Dr. Benjamin Musuku for advising me through this thesis and helping me during my work in Kevitsa. Thank you to Professor Rodrigo Serna for supervising my thesis and teaching me in the field of minerals processing. Additionally, special thanks to Toni Mattson from Metso who helped me conduct the surveys in this thesis and who taught me to use the HSC software.

Lastly, I am grateful for the support from my partner, family and friends during my studies.

Sodankylä, October 2025

Lassi Pekkanen

Table of contents

Preface and acknowledgements	v
Symbols and abbreviations.....	3
Symbols	3
Abbreviations	4
1 Introduction	5
2 Literature review	7
2.1 Flotation	7
2.2 Flotation mechanics.....	7
2.2.1 Collision	8
2.2.2 Attachment and detachment	9
2.3 Flotation reagents	10
2.3.1 Collectors	10
2.3.2 Frothers	12
2.3.3 Other reagents	13
2.4 Particle size distribution	13
2.5 Flotation technologies.....	15
2.5.1 Mechanical flotation cell	15
2.6 Fine particle flotation technologies	18
2.6.1 Flocculation	18
2.6.2 Jameson cell	19
2.6.3 Column flotation cell	21
2.6.4 Reflux Flotation Cell	22
2.6.5 Metso Concorde Cell™	23
2.7 Flotation circuits	25
2.7.1 Flotation efficiency	26
2.8 Problems with fine particle flotation	27
2.8.1 Problems with coarse particles.....	29
2.8.2 Flotation of sulphide minerals	30
3 Research material and methods.....	31
3.1 Kevitsa mill flowsheet	31
3.2 Kevitsa mill sampling campaign.....	32

3.2.1	Sampling campaign equipment.....	32
3.2.2	Sampling campaign procedure.....	33
3.2.3	Mass balancing	36
3.3	Recovery by size	37
4	Results	38
4.1	Scenario 1	38
4.1.1	Mill stability in scenario 1	38
4.1.2	Scenario 1 results	38
4.2	Scenario 2.....	39
4.2.1	Mill stability in scenario 2	39
4.2.2	Scenario 2 results.....	40
4.3	Scenario 3.....	40
4.3.1	Mill stability in scenario 3	40
4.3.2	Scenario 3 results.....	41
4.4	Scenario 4.....	41
4.4.1	Mill stability in scenario 4	41
4.4.2	Scenario 4 results	42
4.5	Size by size recovery.....	42
4.5.1	Scenario 1.....	42
4.5.2	Scenario 2	43
4.5.3	Scenario 3	44
4.5.4	Scenario 4	44
4.6	Summary	45
4.6.1	Flotation circuit stability	46
4.6.2	Survey results summary	46
4.6.3	Size-by-size results summary	48
5	Conclusions	51
	References.....	54
	APPENDIX.....	58

Symbols and abbreviations

Symbols

P_c	Probability of bubble-particle collision
D_b	Bubble size
D_p	Particle size
Re	Reynolds number
$\gamma_{s/a}$	Surface tension between solid and air
$\gamma_{s/w}$	Surface tension between solid and water
$\gamma_{w/a}$	Surface tension between water and air
$W_{s/a}$	Work of adhesion in solid-air interface
N_p	Number of particles in liquid
Z	Number of collisions
E	Flotation collection efficiency
N_b	Number of bubbles
d_p	diameter of particle
d_b	diameter of bubble
G	Shear rate in liquid
Re_b	Bubble Reynolds number
ϵ_g	Superficial gas velocity
Q_g	Gas rate

Abbreviations

AMD	Acid-mine-drainage
ROM	Run-of-mine
CMC	Carboxymethyl cellulose
RFC	Reflux flotation cell
MFF	Metallurgical Flotation Feed
CFC	Copper Final Concentrate
CST	Copper Scavenger Tail
NFC	Nickel Final Concentrate
NiT	Nickel Flotation Tail
NRC	Nickel Rougher Concentrate
NRT	Nickel Rougher Tail
NSC	Nickel Scavenger Concentrate
NCT	Nickel Cleaner Tail
NC4C	Nickel Cleaner 4 Concentrate
NC2C	Nickel Cleaner 2 Concentrate
NC3T	Nickel Cleaner 3 Tail
NFF	Nickel Flotation Feed
NSF	Nickel Scavenger Feed
NC1F	Nickel Cleaner 1 Feed
NC1-1C	Nickel Cleaner 1 Cells 1-2 Concentrate
NC2F	Nickel Cleaner 2 Feed
NC2T	Nickel Cleaner 2 Tail
NC3F	Nickel Cleaner 3 Feed
NC3C	Nickel Cleaner 3 Concentrate
NC4T	Nickel Cleaner 4 Tail
NC1-1T	Nickel Cleaner 1 Cells 1-2 Tail
NC1-2C	Nickel Cleaner 1 Cells 3-6 Concentrate
NCNF	Concorde Cell™ Feed
NCNC	Concorde Cell™ Concentrate
NCNT	Concorde Cell™ Tail

1 Introduction

Demand for metals in the last few decades has increased dramatically, this has led to increase in metals production to meet the demand. The increase in metal demand and improvements in extraction technologies has resulted in high metal production, leading to near-depletion of high-grade ores. (Calvo et al., 2016) As a consequence of high metal production, mineral deposits have become scarce and are usually of low grade, finely disseminated and complex. More complex ore bodies require finer grinding to separate valuable minerals from the host rock (Yáñez et al., 2024). Due to advances in finer grinding, flotation of fine particles has become particularly important in allowing these low-grade mineral deposits to be extracted economically. In addition, mine tailings often consist of fine particles and environmental concerns have been a critical issue in mining industry for many decades. Large surface area of the fine particles leads to higher reaction rates which lead to acid mine drainage (AMD). This has also motivated the mining companies to find technologies to improve recovery of these problematic portions like arsenic and sulphur before storing the tailings. (Farrokhpay et al., 2021)

In flotation processes the feed is ground into a specific top size. Depending on the research done to the specific ore type d_{90} typically varies from 75-150 microns. Even though the top size is relatively high, the feed still consists of a wide range of different particle sizes essentially from zero microns upwards. (Jameson, 2010b) Traditional mechanical flotation cells are able to recover particle sizes of 20-150 microns effectively (Jameson, 2010a). These traditional mechanical flotation cells have been in use in the industry for decades and have been developed to be very efficient (Fuerstenau et al., 2009). To improve mineral recoveries, several different flotation technologies have been investigated and developed in the last two decades (Farrokhpay et al., 2021).

Research shows that fine particle flotation requires different hydrodynamic and reagent concentration during flotation. Fine particles have a high surface area which could lead to more chemical usage to make particles floatable. More importantly fine particles have less collisions with the bubbles and are less efficient in attaching to the bubbles. (Farrokhpay et al., 2021) With coarse particles, particle inertia is the dominating factor, and particles are efficiently colliding with bubbles and attaching to the bubbles without detaching. Fine particles, however, are easily affected by viscous drag effects. Fine particles tend to follow the streamlines of the bubble and probability of a collision is reduced. This effect is amplified with ultra-fine particles. (Jameson, 2010b)

Most fine particle flotation technologies are developed to increase the collisions between particles and bubbles. (Farrokhpay et al., 2021) In 2021 Metso launched the Concorde Cell™ (Yáñez et al., 2024). Concorde Cell™ is a forced air pneumatic flotation cell. Pre-aerated feed is fed into the cell at supersonic velocities which increase the shear rate in the suspension of bubbles and particles. The cell can produce high grade concentrates by recirculating part of the tailings to the feed. (Jameson, 2010b)

2 Literature review

2.1 Flotation

Flotation is a common and cost-effective physico-chemical separation process for minerals. In mineral industries it is used to separate valuable particles in pulp, often minerals from the less valuable gangue particles. It separates the particles using gas bubbles based on the surface hydrophobic or hydrophilic properties. Hydrophobic particles are attached to the gas bubbles and carried to the surface of pulp as froth. Oftentimes different flotation reagents are used to achieve this process and optimise it. (Prakash et al., 2018) (Wills & Napier-Munn, 2006)

Main task of flotation machines or cells is to keep the particles in suspension, disseminate bubbles to the pulp and have enough agitation so that bubble-particle attachment can take place without detachment until froth is collected in the concentrate launders. (Liu & Schwarz, 2009)

2.2 Flotation mechanics

In flotation hydrophobic minerals are collected from the pulp by bubbles. There are three steps for the particle to be collected: collision, attachment and stability as shown in figure 1.

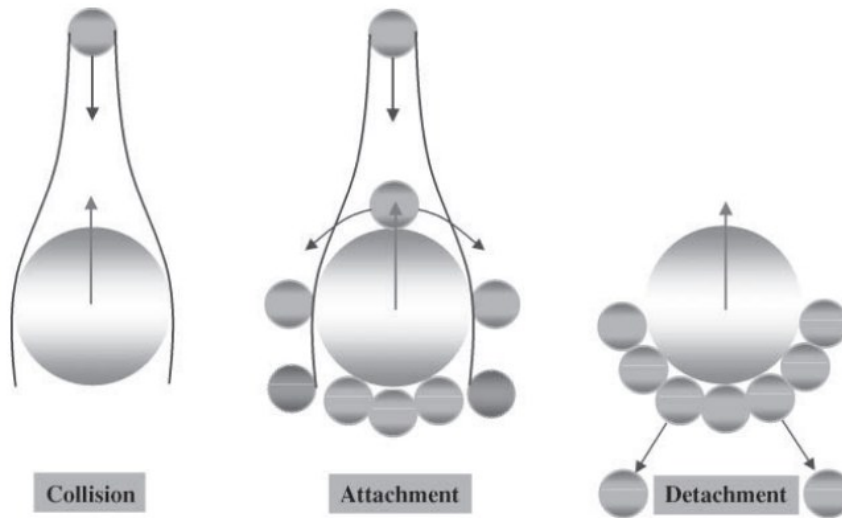


Figure 1. Collision, attachment and detachment of a particle and bubble. (Tao, 2005)

2.2.1 Collision

Air bubbles and solid particle interactions, and their movements, are the most important phenomena in flotation. (Liu & Schwarz, 2009) Flotation of a particle starts with a process of bubble-particle collision. It is where a particle collides with a bubble because of a sufficiently close encounter. The probability of a collision (P_c) for intermediate size and Reynolds number of bubbles can be calculated with equation 1.

$$P_c = \frac{3}{2} \left[1 + \frac{\left(\frac{3}{16}\right) Re^{0,72}}{1 + 0,249 Re^{0,56}} \right] \left(\frac{D_p}{D_b}\right)^2 \quad (1)$$

Where D_b is the bubble size, D_p is the particle size and Re is the Reynolds number.

Equation 1 shows that when the probability of a collision increases to the square of the ratio of particle size to bubble size. It suggests that probability of collisions are increased when particle size is increased and bubble size is reduced. (Tao, 2005)

2.2.2 Attachment and detachment

When particle and bubble collide, attachment does not occur instantly (Wills & Finch, 2016). Attachment is determined by hydrodynamic and surface forces of the particle and bubble. For the particle to be able to rupture the thin film surface tension of bubble-liquid interface it needs to be hydrophobic enough.

Forces that are holding the particle to the bubble are shown in figure 2 and 3.

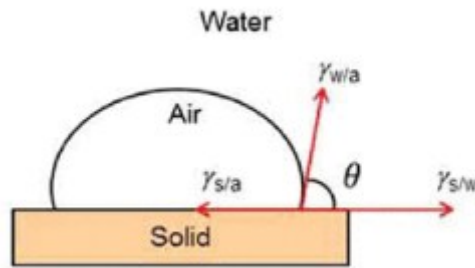


Figure 2. Forces holding a flat solid-air interface. (Wills & Finch, 2016)

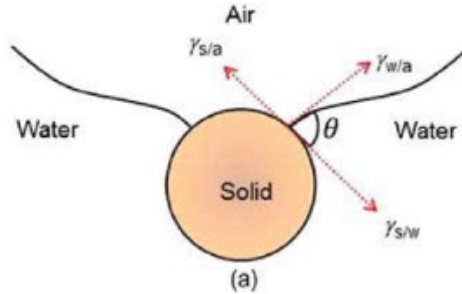


Figure 3. Forces holding a round solid-air interface. (Wills & Finch, 2016)

Tensile forces develop an angle between the particle surface and the bubble surface. Equation 2 shows surface tensions at equilibrium.

$$\gamma_{s/a} = \gamma_{s/w} + \gamma_{w/a} \cos\theta \quad (2)$$

Where $\gamma_{s/a}$ is the surface tension between solid and air, $\gamma_{s/w}$ is the surface tension between solid and water, $\gamma_{w/a}$ is the surface tension between water and air and θ is the angle between the mineral surface and the bubble.

Work of adhesion $W_{s/a}$ is a force that is required to break the bubble-particle attachment. It is equivalent to the work required to break the solid-air interface and to create new water-air and solid-water interfaces. Work of adhesion is represented in equation 3.

$$W_{s/a} = \gamma_{w/a} + \gamma_{s/w} - \gamma_{s/a} \quad (3)$$

Combining equations 1 and 2 provide the calculation for work of adhesion shown in equation 4.

$$W_{s/a} = \gamma_{w/a}(1 - \cos\theta) \quad (4)$$

This shows that with a greater contact angle between particle and bubble, the greater the work of adhesion is needed to break this connection. This also means that the particle is less prone to disruptive forces when the contact angle is large. (Wills & Finch, 2016)

2.3 Flotation reagents

Flotation reagents are classified by their purpose in the process. Main flotation reagents are collectors, frothers, depressants, modifiers and flocculants. (Somasundaran & Wang, 2006)

2.3.1 Collectors

Collectors are used to make the mineral surfaces hydrophobic. Only a few minerals such as coal and molybdenite are naturally hydrophobic. (Hanumantha Rao & Forssberg, 1997) Collectors are usually organic compounds which coat mineral surfaces making the mineral particle hydrophobic. These collectors consist of nonpolar hydrophobic group and a polar minerophilic group. Minerophilic group determines the ability of the collector reagent to

react with the mineral surface. Collector reagents can interact with mineral surfaces by physical adsorption, chemisorption or chemical reactions due to differences in dissociation, solubility or polarity of the reagent. The minerophilic portion consists of a linking atom, bonding atom and a cationic ion as shown in figure 3. (Somasundaran & Wang, 2006)

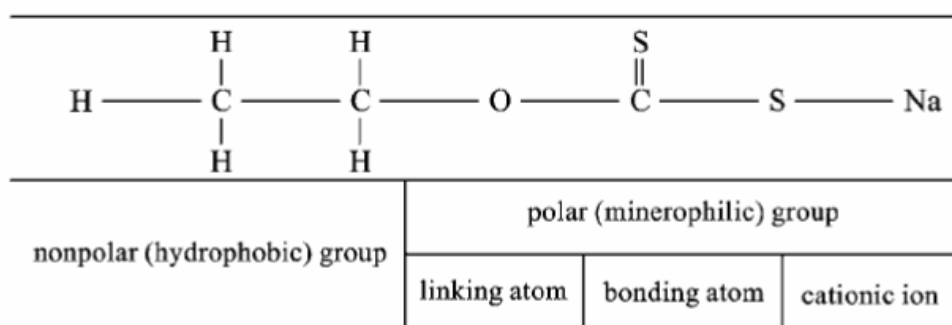


Figure 4. Chemical composition of a collector molecule. (Somasundaran & Wang, 2006)

Collectors are added to the pulp and time is allowed before flotation occurs to allow collector adsorption to the mineral surface. This time is known as conditioning period. (Wills & Napier-Munn, 2006) The collector adsorbs the polar minerophilic group to the mineral particle surface and orients the non-polar hydrophobic group towards the water phase. The hydrophobic effect of the collector is affiliated with the structure and length of the nonpolar hydrophobic group. (Bulatovic, 2007)

Collectors are usually divided into ionizing and non-ionizing type. Non-ionizing collectors are hydrocarbon compounds that are insoluble in water. They are believed to form a thin film on the mineral surface which makes the mineral hydrophobic. On the other hand, ionizing collectors are a larger group of collectors, and they are divided into anionic and cationic collectors.

Anionic collectors are most widely used in flotation processes. It includes collectors with a carboxyl group, collectors with sulfuric acid anion, xanthogenate type collectors and dithiophosphate collectors. Cationic collectors

commonly include a nitrogen group with unpaired electrons present. They often have a positive charge in aqueous environments. (Bulatovic, 2007)

2.3.2 Frothers

Frothers are surface-active reagents containing a polar group and a hydrocarbon radical. They are capable of adsorbing in the air-water interface. Frothers are used in flotation to make the froth stable, disseminate the gases and to accelerate the flotation process. At the surface of the pulp, air bubbles need to be able to form a stable froth to support the mineral particles, otherwise the bubble will burst and the mineral particle is lost back to the pulp (Wills & Finch, 2016).

Frother molecules arrange at the air-water phase so that the non-polar group is orientated in the gas phase and the polar group is orientated at the liquid phase. This orientation prevents bubbles from colliding which prevents bubble collapsing and coalescing.

Frothers are commonly divided into groups by their properties and behavior in different pH values. They are divided into acidic, neutral or basic. Acidic frothers have the best efficiency in acidic solutions. Typical acidic frothers include phenols and alkyl sulphates. Acidic frothers have been widely used until the 1960s but has been diminishing due to environmental concerns. Neutral frothers are the largest group out of these and most widely used in industry. Neutral frothers are efficient in both acidic and alkaline solutions. They can be divided into six different groups that have large differences in their chemical composition. The groups are aliphatic alcohols, cyclic alcohols, alkoxy paraffins, polyglycol ethers, polypropylene glycol ethers and polyglycol glycerol ethers. Basic frothers are represented by pyridine and homologs which are recovered as by-products from coal tar distillation. They can be used in base-metal ore or oxide lead minerals flotation processes. (Bulatovic, 2007)

2.3.3 Other reagents

Other chemicals used in flotation include modifying reagents. Modifying reagents have a large variety of functions. Modifiers can react with the mineral surfaces changing their chemical composition or cleaning their surfaces of any coatings. They are also capable of changing the floatability of minerals and change the pH of the pulp. Modifiers can be divided into inorganic and organic groups. Inorganic modifiers are often used for changing the pH in the pulp but some of them can also be used in fine particle flocculation. Most widely used inorganic modifiers include sulfuric acid and lime which are used in pH control. (Bulatovic, 2007)

Organic modifiers include organic polymers and organic acids. Organic polymers include a large variety of complex polymers. They can be used as dispersants, flocculants and depressants. These polymers can be divided into four groups: non-ionic, cationic polymers and anionic polymers. Non-ionic polymers contain starches, dextrans, tannic acid derivatives and oxycellulose. Anionic polymers include carboxymethyl cellulose (CMC), cellulose gum and lignin sulfonates which are widely used in the industry as depressants. Cationic polymers include Ethylenediamine, Diethylenetriamine, polyamines substituted dithiocarbamates or amino acids such as β -alamine. Anionic polymers are widely used in the industry as depressants which depress some magnesium bearing minerals and pyrrhotite in copper-nickel bulk flotation. (Bulatovic, 2007)

2.4 Particle size distribution

Analysing particle size distribution is important in determining the quality of grinding and the degree of liberation of the valuable minerals from the gangue materials. Particle size analysis is often done with sieves arranged in a stack with the coarsest sieve on the top and finest at the bottom. Weight of material each sieve has captured are gathered in a table. With the collected

weights a particle size distribution (PSD) graph is produced, which can be seen in figure 5.

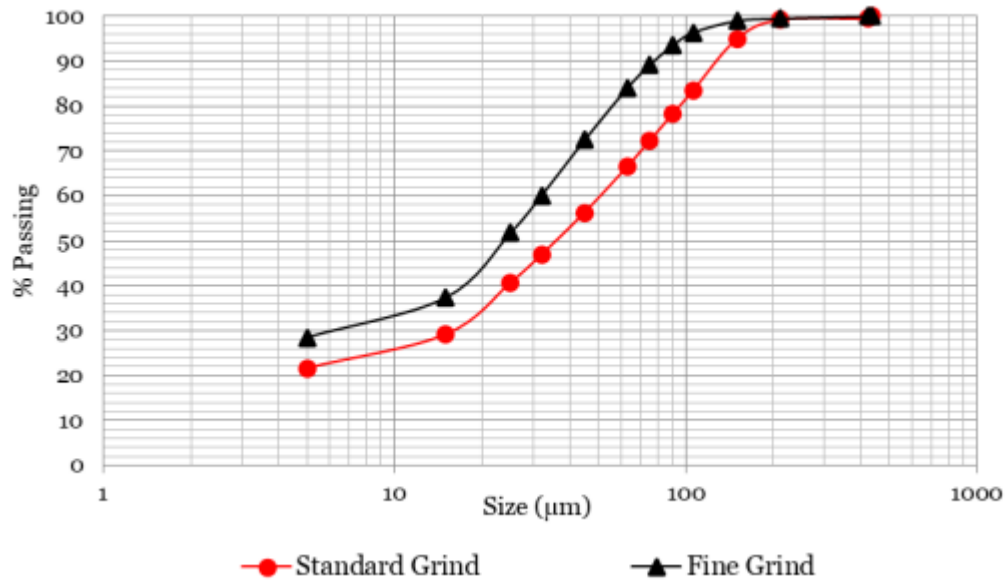


Figure 5. PSD graph of Kevitsa mill. (Musuku, 2024)

Nowadays industrial processes often use an on-line particle size analyser. These on-line analysers use different sensors to determine the PSD of the slurry. The on-line analysers allow for rapid response from plant operators to changes in the grinding process. (Wills & Napier-Munn, 2006)

To achieve high grinding efficiency, effective classification is needed, one that produces narrow size distributions that are suitable for flotation. Fine grinding circuits cause poor classification causing higher energy consumption, produce too much ultrafine particles and have a poor control of top size particles. (Pease et al., 2006)

A key challenge in optimizing flotation performance is understanding the effect of PSD. PSD plays a crucial role in froth stability and flotation performance. Even small variations in PSD can impact froth stability and flotation performance. With a broad PSD froth stability is enhanced as fine particles

coat bubble surfaces and reduce coalescence, while coarser particles provide structure. However, too many fine particles can lead to dense froth that contains water and gangue, reducing the concentrate grade and recovery. (Norori-McCormac et al., 2017) Fine particles have a high surface area and are highly reactive, sensitive to oxidation and surface precipitation. (Pease et al., 2006)

2.5 Flotation technologies

Flotation has been in industrial use for many decades. Mechanical flotation cells operational principles have changed little since their invention in 1912, but their maximum size has increased greatly during the last few decades. In the past 50 years new technologies such as pneumatic column flotation cells and high-intensity flotation cells have been researched and commissioned. (Fuerstenau et al., 2009)

2.5.1 Mechanical flotation cell

Most of the mechanical flotation cells consist of a tank with an agitator. Agitator helps to keep particles in suspension in the slurry and disperses air into bubbles. It creates an environment in the cell where particle-bubble attachment can occur. Attached particles travel upwards to the top of the cell where concentrate is collected into a launder. Particles that are not attached to bubbles flow out of the bottom of the cell.

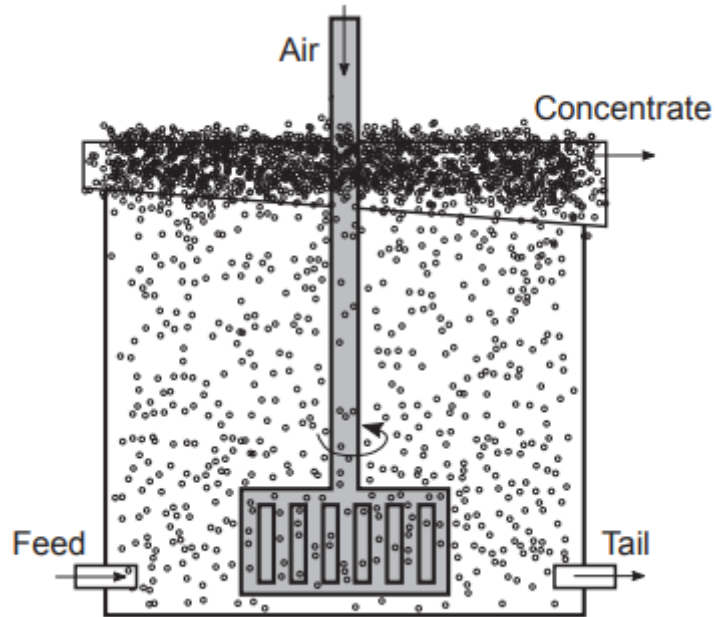


Figure 6. Drawing of a mechanical flotation cell. (Mesa & Brito-Parada, 2019)

Mechanical flotation cells can be divided into three hydrodynamic zones. The first zone is located close to the agitator. It is a turbulent zone which is necessary for suspension of solids, dispersion of air into bubbles and particle-bubble interaction occurs. The second zone lies the quiescent zone. The quiescent zone is a less turbulent region where particle-bubble aggregates rise. This zone reduces the amount of gangue minerals entrained between bubbles. Third zone above the quiescent zone is the froth zone. It helps cleaning the concentrate and improves the grade of the concentrate.

Gas dispersion is an important part of mechanical flotation cells. To generate bubbles in a mechanical cell air cavities are first formed at the trailing edge of the agitator, which is a low-pressure region. Secondly bubbles form by the shedding of vortices at the tail of the cavity.

Air can enter the flotation cell in one of two ways. The first option is to use a blower which forces low pressure air through the axle of the agitator into the bottom of the cell. The second option is to use self-induced air entry

where air is sucked into the cell by vortexing. With the blower design the agitator is located at the bottom of the cell, whereas with the self-induced air entry model the agitator is located around the midpoint of the cell. (Fuerstenau et al., 2009)

Over the last few decades flotation cells have become substantially larger. This is due to the increase in demand for higher throughput in processing plants. Rather than increasing the amount of equipment, flotation equipment size has become larger to meet these throughput demands. Having fewer number of cells offers technical and economic advantages. However, when scaling up cells, fluid dynamic properties alter the performance of the flotation cells. Pulp dynamics are affected by speed, shape and size of the agitation mechanism. On top of that the distance the froth must travel to the cell lip is longer with bigger flotation cells.

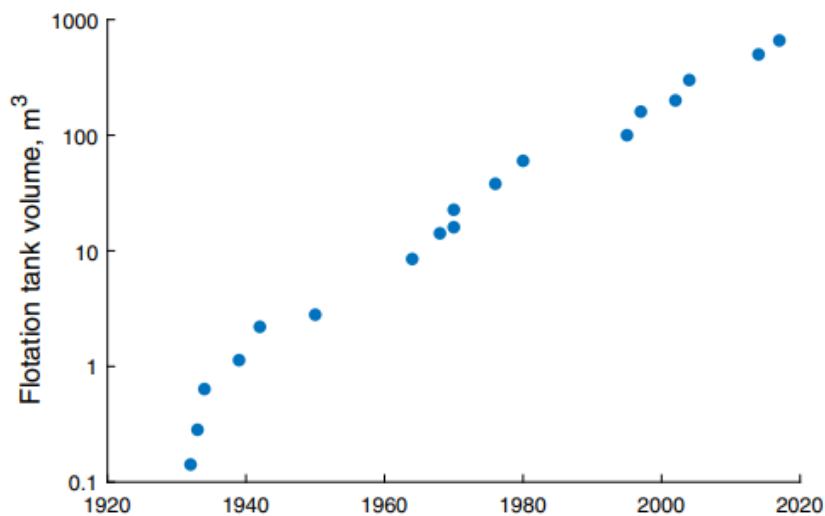


Figure 7. Maximum flotation tank volumes over the year. (Mesa & Brito-Parada, 2019)

In Metso Tank Cell produced froth overflows into launders where they are easily transported forwards. Unwanted minerals, tailings, exit the tank at the bottom of the tank. Air is delivered to the cell through the hollow shaft and is dispersed with the impeller and stator. Typically, mechanical cells are

arranged in series where tailings from the first cell move on to the next and so on. Concentrates from a series of cells may be treated as final concentrate or moved on to series of cleaner cells depending on the requirements of the circuit. Mechanical cells have been developed to be highly efficient through many years of operation. (Fuerstenau et al., 2009)

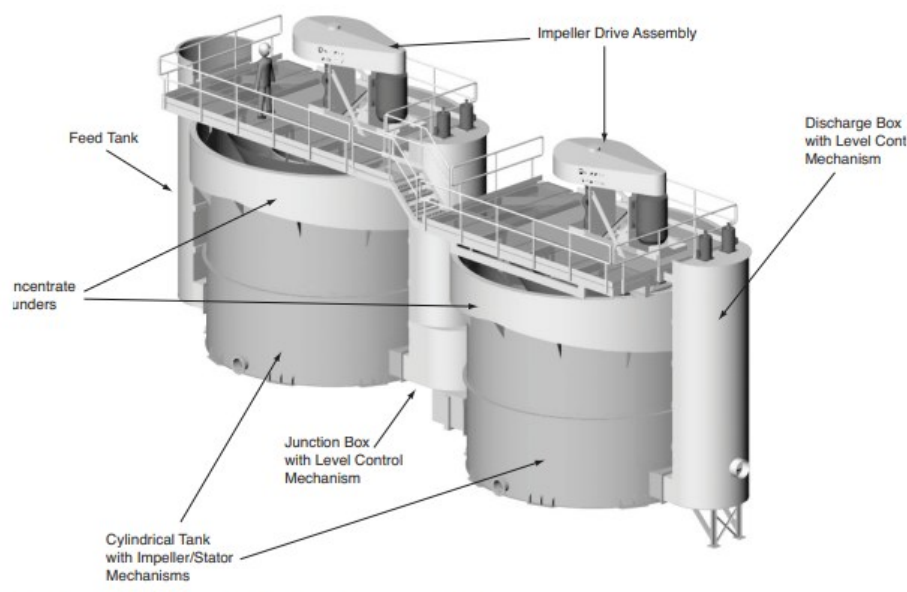


Figure 8. Picture of two Metso TankCells. (Fuerstenau et al., 2009)

2.6 Fine particle flotation technologies

New flotation technologies for fine particle flotation have been developed in the recent years. Most of them are designed to increase the particle-bubble collision frequency. (Farrokhpay et al., 2021)

2.6.1 Flocculation

One effective approach to overcome low collision and attachment efficiencies of fine particles with air bubbles is to use flocculation. Flocculation involves the aggregation of fine particles into larger clusters, making them behave more like coarse particles in flotation. With flocculation particles have

greater inertia which reduces their tendency to follow streamlines around bubbles, it improves particle-bubble collision efficiency, and it improves particle-bubble attachment efficiency.

Flocculation can be achieved with electrolyte addition, pH adjustment or polymer addition. High molecular weight polymers such as polyacrylamides adsorb on particle surfaces linking them into flocs. This has been achieved with minerals such as hematite, quartz and some laterites. With pH adjustment electrostatic aggregation is achieved. It controls the surface charge of particles. Aggregation is maximized at the isoelectric point which is the pH where net charge is zero. Hydrophobic aggregation can be achieved with highly hydrophobic particles. This mechanism can be enhanced with selective collector adsorption, making targeted particles more prone to agglomerate.

In fine particle flotation selective flocculation is often desired. Selective flocculation aims to aggregate valuable particles only, leaving gangue particles dispersed. This is achieved by using selective flocculants that adsorb only to the desired mineral surfaces and hydrophobization of desired mineral surfaces before flocculant addition. This method has been successfully applied in hematite-silica separation, low grade copper ores and lateritic nickel ores. These flocculated flocs can be directly floated, or carrier flotation can be applied. Carrier flotation is a process where fine particles attach to coarser carrier particles which enhance collisions with bubbles.

For industrial scaling flocculation is still challenging due to poor selectivity and high cost. (Farrokhpay et al., 2021) (Miettinen et al., 2010)

2.6.2 Jameson cell

Jameson flotation cell was developed by Professor G.J. Jameson in collaboration with Mount Isa Mines in 1986 and is widely used in industry.

Jameson cells design is based on having large number of fine bubbles which have a large surface area. (Prakash et al., 2018)

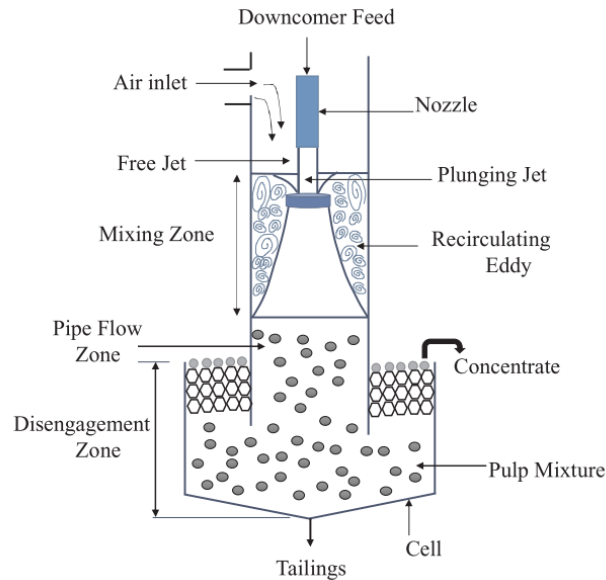


Figure 9. Drawing of a Jameson cell. (Prakash et al., 2018)

Jameson cell consists of three main parts: downcomer, tank pulp zone and tank froth zone. Feed is pumped to the downcomer through an orifice plate to produce a high-pressure jet. Air is introduced to the jet through an inlet by vacuum effect and is entrained to the pulp. The downcomer is the main area of bubble-particle collisions.

Pulp zone is the second area of bubble-particle collisions and where bubbles disengage from the pulp. Aerated mixture exits the downcomer and enters the flotation tank. velocity and a large density difference result in recirculating patterns which result in particles being able to stay suspended.

Froth zone is where collected particles are gathered. Froth washing system remove entrained gangue and concentrate is collected to launders. The cell is insensitive to tank residence time but is affected by residence time in the downcomer. (Harbort et al., 2003)

2.6.3 Column flotation cell

Column flotation is in wide use in mineral processing industry. Column flotation cell is a tall cylindrical tank with no agitation. In column flotation, slurry is introduced near the middle or the bottom of the cell. Air is introduced usually via sparger from the bottom of the cell. This creates a counter current where air bubbles are rising up and slurry is descending the cell. This configuration creates conditions where particle-bubble collisions and attachment occur for extended time compared to typical mechanical flotation cells. In addition, fine bubbles increase the probability of collision and attachment due to their higher surface area and slower rising velocity.

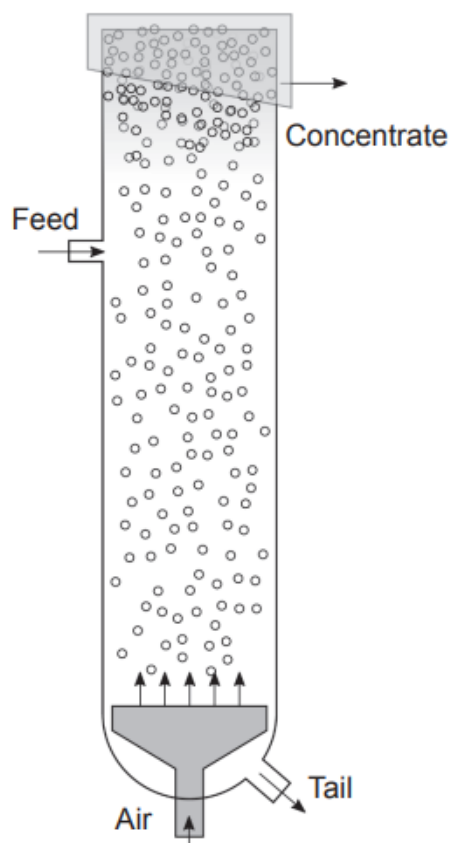


Figure 10. Drawing of a column flotation cell. (Mesa & Brito-Parada, 2019)

Separation process of particles happens in two distinct zones in the column flotation cell. First is the Collection zone where particles collide and attach to the bubbles. Absence of agitation leads to less turbulent environment, leading to less detachment and allowing more effective fine particle recovery. Second is the froth zone where stable froth is formed. Wash water is introduced to the top of the froth zone, creating a downward flow removing entrained gangue particles, enhancing recovery and improving the concentrate grade. (Prakash et al., 2018) (Fuerstenau et al., 2009)

2.6.4 Reflux Flotation Cell

Reflux flotation cell (RFC) was designed in the university of Newcastle and it combines previous inventions from the minerals processing industry. At the bottom of the cell is an inclined channel adapted from a reflux classifier. Top of the cell is a combination of previous technologies having a reverse fluidized bed and a downcomer similar to a Jameson cell. (Chen et al., 2022)

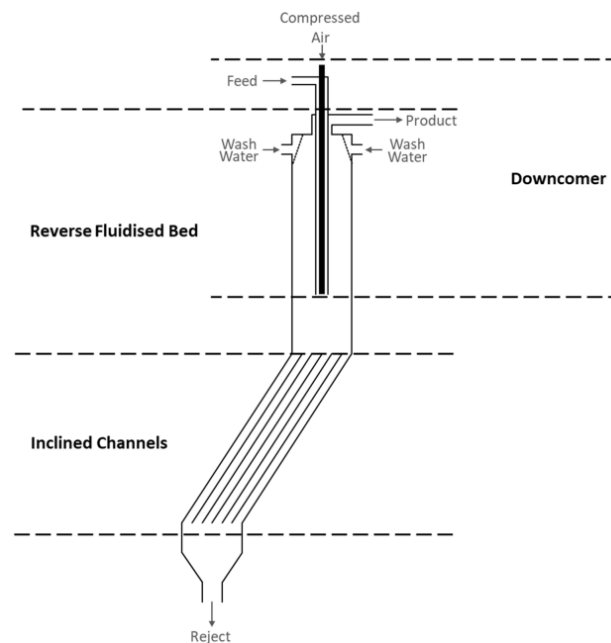


Figure 11. Drawing of a reflux flotation cell. (Chen et al., 2022)

In the RFC downcomer high feed flowrate generates and mixes fine bubbles with the slurry feed. Different to the Jameson cell RFC uses an annular microhole sparger in the downcomer to generate these bubbles.

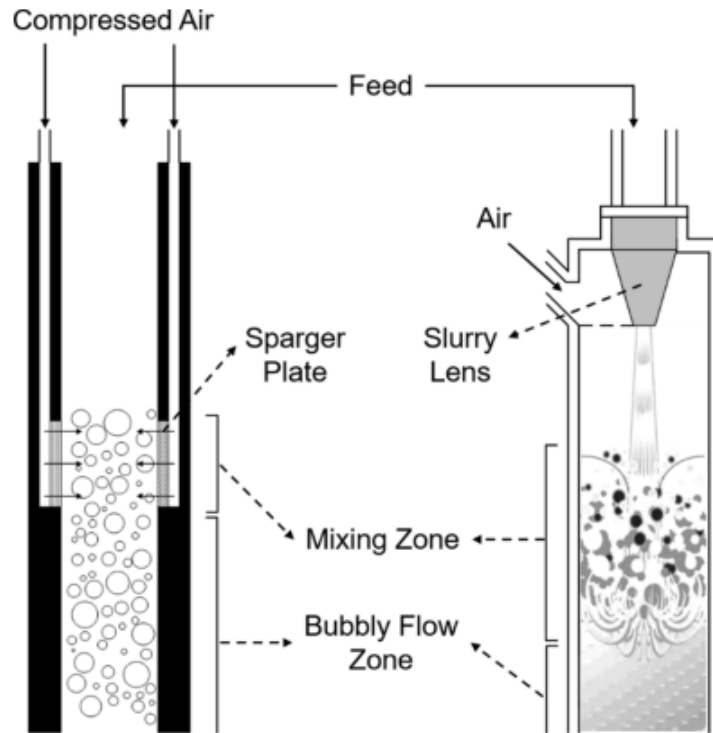


Figure 12. Drawing of the reflux flotation cell downcomer. (Chen et al., 2022)

Major function of the reverse fluidized bed in the RFC is to create a bubbly zone instead of a froth layer that is done in conventional flotation cells. This is achieved by introducing wash water at the surface downwards. This helps to remove the effect of gangue minerals being carried to the concentrate and improves flotation performance also with coarse particles.

Inclined channels in the RFC enhance the separation of non-attached particles and bubbles with attached hydrophobic particles. (Chen et al., 2022)

2.6.5 Metso Concorde Cell™

The Concorde Cell™ is an enhanced forced-air pneumatic flotation technology. It was launched as a product by Metso in 2021. It is dedicated to

recovering fine and ultrafine particles. The cell relies on high shearing, high energy dissipation and fine bubbles to improve recovery. (Yáñez et al., 2024)

The Concorde Cell™ is shown in Figure 13. In the Concorde Cell™, the feed enters the Blast tube as a vertical jet through a choke. Pressurized air is fed into the blast tube after the first choke where it mixes with the feed. The aerated feed mixture then enters the cell through the second choke at the speed of sound, approximately 20 m/s. After the second choke shockwave is created and there is a large change in pressure over a small distance. Due to this pressure change the size of the bubbles is reduced markedly.

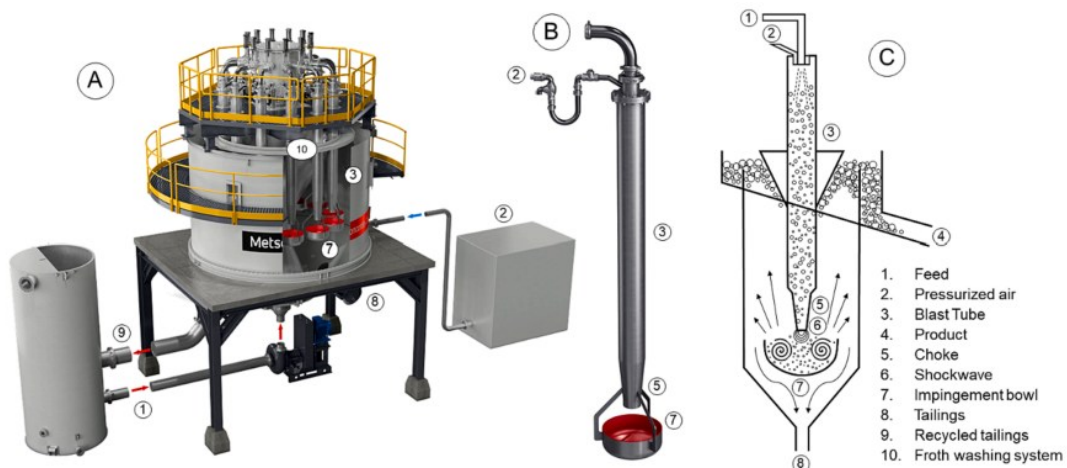


Figure 13. A: 3D render of Concorde Cell™ equipped with 12 Blast Tubes, B: 3D rendering of a single Blast Tube, C: Diagram of the Concorde Cell™. (Yáñez et al., 2024)

There are three locations where particle-bubble interactions can occur: inside the Blast tube, in the shockwave after the second choke or in the vortex ring formed by the impingement bowl. (Jameson, 2010b)

Total residence time of the valuable particles inside the Blast tube can be increased by recirculating part of the tailings back to the feed. This gives the particles more opportunities to be collected which enhances the total

recovery of the cell. However, increasing the recirculating load of the cell reduces the amount of fresh feed into the cell. (Jameson, 2010b)

Because fine particles are easily entrained, Concorde Cell™ can be equipped with a froth washing system. Froth washing removes entrained gangue from the froth, dilutes the pulp and breaks down the froth. Froth washing is done by spraying water above the froth. This creates a downward liquid flow through the froth. (Yáñez et al., 2024)

2.7 Flotation circuits

Industrial flotation circuits are a continuous process where cells are arranged in series and parallel. Pulp enters the first cell of the series and part of the valuable material is floated as froth, pulp that is not floated in the first cell move on to the second cell and so on. Cells are typically equipped with weir type level controls or dart valves. Height of the froth column is determined by adjusting the tailings flow.

In the first cell of the series called rougher cells, grade of valuable minerals is high so froth depth can be kept low. Froth column level is decreased from cell to cell as the pulp becomes depleted from valuable floatable particles. Last cells in series contain relatively low-grade froths and these cells are called scavenger cells. Product of scavenger cells is often recirculated to the start of the system. Although excessive circulating loads should be avoided to not dilute the rougher cells feed and reduce the flotation time. Figure 14 shows typical flotation circuit.

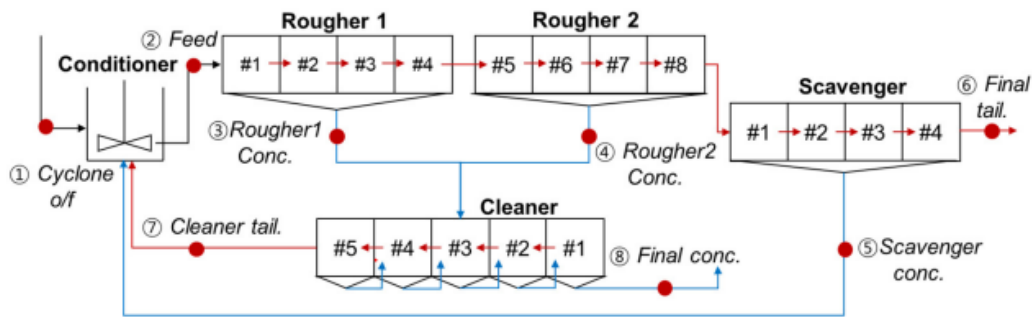


Figure 14. Flowsheet of a typical flotation circuit. (Han et al., 2021)

Concentrate from the rougher cells are often refloated in cleaner cells, where froth depths are kept low to produce high grade concentrates. Tailings from the cleaner cells are often recirculated into the rougher cells. This kind of flotation circuit is often employed when gangue minerals tend to also float and is difficult to separate from the valuable minerals. With this kind of circuit dilution water used in cleaner flotation can be harmful when it enters back into the rougher flotation because it effects the pulp ratio in the rougher stage.

When selecting a flowsheet to a flotation plant, the grain size of the flotation feed is the major consideration. This is due to flotation response being dependant on the level of liberation of the minerals in the ore. (Wills & Napier-Munn, 2006)

2.7.1 Flotation efficiency

Flotation performance is often represented by using grade-recovery curves. However, these curves are often sensitive to variations in feed grade and feed rate. This makes comparing plant performance and operating conditions difficult. Changes in feed rate and grade are common in industrial applications and can shift these curves significantly. This makes it difficult to determine whether variations in the curve are due to changes in the process or fluctuations in the feed. (Neethling & Cilliers, 2012)

2.8 Problems with fine particle flotation

Flotation of particles in the size of 20-150 microns is known to be successful. Fine particles under the size of 20 microns require different hydrodynamic and chemical conditions during their conditioning and flotation. Key parameters in fine particle flotation are bubble size, particle aggregation and flow conditions. Weak recovery of fine particles is often caused by low particle-bubble collision as these particles often follow the fluid streamlines around the rising bubbles due to the small mass of fines. Additionally fine particles have a larger surface area, so they are more prone to surface oxidation and require more chemical dosing.

It has been observed that entrainment occurs in fine particle flotation more often than with coarse particles. Entrainment is a mechanical process where fine particles of less than 20 microns are entrained in the wake of a rising bubble but are not attached to the bubble. This can lead to gangue minerals getting into the froth and be collected to the concentrate and results in poor mineral separation. (Farrokhpay et al., 2021) In figure 15 the so called “elephant curve” is shown.

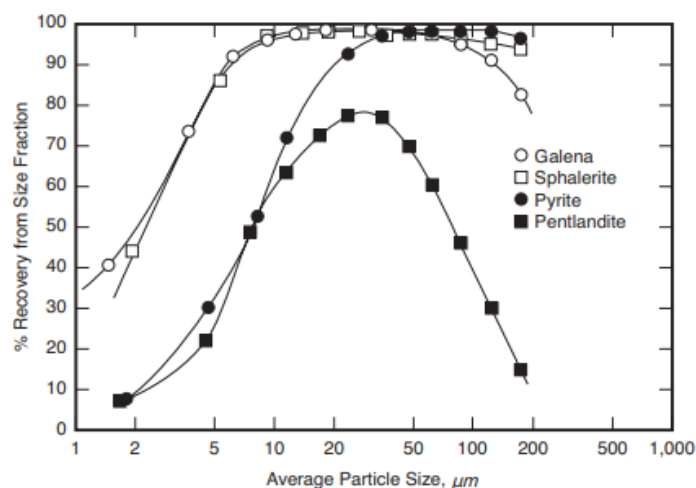


Figure 15. Graph of recoveries by particle size for different minerals. (Fuerstenau et al., 2009)

It shows that most of the minerals have decreased recovery in fine particle sizes. Especially with Pentlandite, recovery with particle sizes under 20 and over 50 microns drop significantly. (Fuerstenau et al., 2009)

Rate of flotation of particles in the pulp phase is expressed in equation 5.

$$\frac{dN_p}{dt} = -kN_p = -ZE \quad (5)$$

Where N_p is the number of particles in the liquid, k is the rate constant s^{-1} , Z is the number of collisions and E is the collection efficiency, which includes efficiencies of detachment and attachment. For the rate of collisions equation 6 can be used.

$$Z = (2/3)N_p N_b (d_p + d_b)^2 G \quad (6)$$

Where N_b is the number of bubbles, d_p and d_b are diameters of particles and bubbles and G is the shear rate in the liquid.

Flotation collection efficiency E can also be presented as in equation 7.

$$E = \left(\frac{d_p}{d_b}\right)^2 \left[\frac{3}{2} + \frac{4}{15} Re_b^{0.72}\right] \quad (7)$$

Bubble Reynolds number is presented in in equation 8.

$$Re_b = \rho_L G d_b^2 / \mu \quad (8)$$

Where μ is the viscosity of the liquid and ρ is the density of the liquid.

To estimate the number concentration of bubbles N_b in equation 6 we can use equation 9.

$$N_b = \frac{6\varepsilon_g}{\pi d_b^3} \propto \frac{Q_g}{d_b^3} \quad (9)$$

Where ε_g is the superficial gas velocity and Q_g is the gas rate.

Combining the previous equations 5, 6, 7, 8 and 9 we can express flotation rate in equation 10.

$$\frac{dN_p}{dt} = -KN_p \propto ZN_p \cdot \frac{Q_p}{d_b^3} \cdot d_b^2 \left(1 + \frac{d_p}{d_b}\right)^2 G \cdot Z \left(\frac{d_p}{d_b}\right)^2 G^{1/2} d_b Z \propto \frac{N_p Q_g d_p^2 G^{3/2}}{d_b^2} \quad (10)$$

This equation demonstrates that the flotation rate is decreased when particle size d_p decreases. It also shows that to counter smaller particle sizes reducing bubble size d_b and increasing the shear rate G increases flotation rate. (Jameson, 2010b)

2.8.1 Problems with coarse particles

The mechanism concerning the issues in coarse particles are different from those of fine particles. Coarse particles, typically larger than 150 μm also suffer from low flotation recovery. This is mainly due to detachment from bubbles in high turbulence conditions, poor liberation which leads to locked particles and low hydrophobicity that reduce their probability of attachment to bubbles.

To prevent detachment, flotation environment needs lower turbulence especially in the froth and separation zones. Improving mineral liberation with improved grinding strategies can also help to release the valuable mineral components, enhancing their flotation response.

2.8.2 Flotation of sulphide minerals

High-grade nickel concentrate production has become increasingly more difficult due to depletion of easily treatable nickel deposits. Pentlandite is a major nickel-sulphide mineral. It is often found in association with quartz and other silicate minerals. Pentlandite is a low-grade nickel ore and fine grinding is needed to liberate nickel particles from the gangue material. With fine grinding pentlandite processing often suffers from entrained gangue particles. To limit this, depressants such as carboxymethyl cellulose (CMC), soda ash or guar gum is used. Figure 16 shows the size by size mineral recoveries in Boliden Kevitsa concentrator.

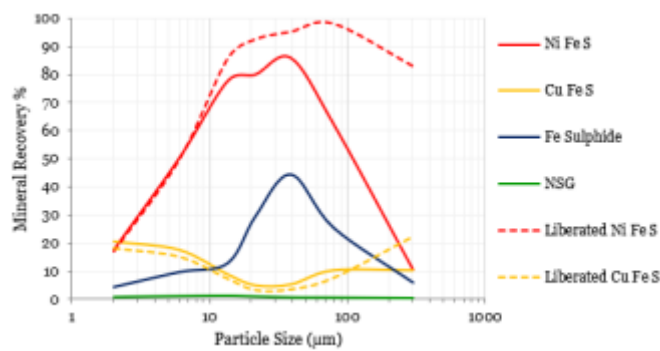


Figure 16. Graph of mineral recoveries by particle size at the Kevitsa mill. (Musuku, 2024)

In Kevitsa, previous research has discovered that much of the losses of liberated pentlandite mineral happen in the fine fraction. Research has also shown that almost 60% of nickel feed is under 25µm. Since the milling circuit uses autogenous milling, ore mineralogy influences the PSD of the flotation feed. (Musuku, 2024)

3 Research material and methods

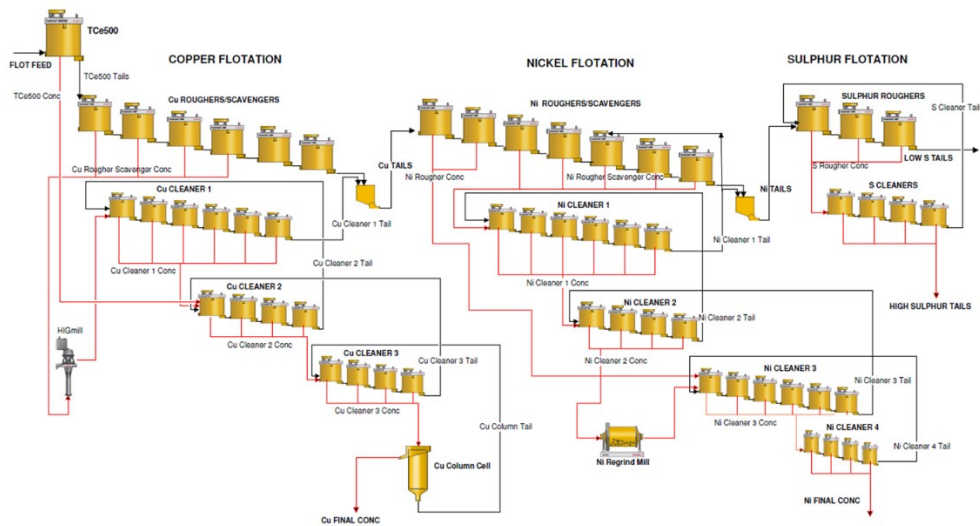
3.1 Kevitsa mill flowsheet

Kevitsa mill consists of four parts: crushing, milling, flotation and de-watering. Run-of-mine (ROM) ore is delivered to a pad where ore is piled into fingers which contain uniform mineral grades and hardness. From the ROM pad ore is loaded to the primary crusher which is a single gyratory crusher. From the primary crusher ore is conveyed to the primary banana screen where under- and oversize fractions are conveyed to the interim storage pile. Midsize fraction is conveyed to the secondary crushers. Secondary crushers are two identical cone crushers. Cone crushers product is also conveyed to the interim stockpile. Stockpile has room for ore for around two days of production. From the stockpile ore is conveyed into three primary fully autogenous (AG) mills. Mill product is screened, and underflow from the screen which is slurry is pumped to hydro cyclones and oversize ore rocks are conveyed to secondary crushing or conveyed to the secondary pebble mill. Hydro cyclones separate coarse particles back to grinding mills and finer particles are fed into flotation.

Flotation consists of three parts: copper flotation, nickel flotation and sulphur flotation. Flotation cells vary from 500 m³ to 16 m³ with most of the rougher and scavenger cells being 300 m³ to 160 m³ and cleaner cells being smaller in size. Copper flotation consists of rougher stage, scavenger stage and 4 cleaner stages. Concentrate fed into copper cleaner stages is re-grinded with a high intensity grinding mill. Final copper concentrate is cleaned with a column flotation cell. Copper scavenger tails are pumped forward as nickel flotation feed. Nickel flotation consists of rougher stage, scavenger stage and 5 cleaner stages. Nickel cleaner circuit also has one ball mill for regrinding. Nickel flotation tails are pumped into sulphur flotation. Sulphur flotation consists of rougher stage and cleaner stage. Sulphur flotation tails are pumped to low-sulphur tailings storage pond and sulphur concentrate is

pumped into high-sulphur tailings storage pond. Copper and nickel concentrates are separately pumped into dewatering where both streams consist of their own thickener. Concentrates are dried with larox pressure filters.

Concorde Cell™ was installed to the nickel circuit, and it can be fed with nickel rougher concentrate (NRC) or nickel cleaner 3 tail (NC3T). Concorde Cell™ in Kevitsa is equipped with one large BlastTube. Only part of the feed stream could be fed into the Concorde Cell™ due to its small size and high circulating load.



3.2 Kevitsa mill sampling campaign

Kevitsa mill sampling campaign was conducted during 10.3.2025-20.3.2025. Samples were taken on 4 days 10.3, 12.3, 19.3 and 20.3. During each sampling day total of 3 rounds of samples were collected per day to reduce errors in results. Ore from the mine was kept the same during sampling campaign and plant performance was kept as stable as possible. Parameters for the Concorde Cell™ were kept the same throughout the sampling campaign.

3.2.1 Sampling campaign equipment

Samples were collected in three different ways (1) from Outotec courier on-site analyser sample streams, (2) directly from concentrate hopper from a bleed valve and (3) with a dip sampler directly from a flotation cell or a feed box. Immediately after sampling all samples were weighed to get slurry densities.

After weighing, samples were filtered with a vacuum filter. Filtered samples were dried in a sample oven overnight. Dry samples were divided into two parts, first part was sent for analysis at external laboratory, Eurofins Labtium Oy, to determine metal assays. Remaining part of the sample was stored while selected samples were also screened for size-by-size chemical analysis for recovery determination.

Process indicator data from on-site x-ray fluorescence (XRF) analyser, density meters and flow meters were used to analyse process stability during sampling.

3.2.2 Sampling campaign procedure

Table 1: Sampling campaign days and number of samples.

Scenario	Rounds	Concorde Cell™	Feed to Concorde Cell™	Samples	Total
1	1-3	ON	NRC	26	78
2	4-6	OFF	-	22	66
3	7-9	OFF	-	22	66
4	10-12	ON	NC3T	26	78

For scenario 1 Concorde Cell™ was in operation and part of NRC was fed into the Concorde Cell™ feed hopper. Total of three rounds of 26 samples were collected, totalling 78 samples during the day.

For scenario 2 Concorde Cell™ was turned off and circuit was stabilized before samples were collected. Scenario 2 was to produce a baseline of plant performance before installation of Concorde Cell™ and to compare what

effects the Concorde Cell™ has to the circuit. For baseline 22 samples were collected per round, and three rounds were collected during the day.

Scenario 3 was again to produce a comparable baseline survey for the fourth day of sampling with a different feed to the Concorde Cell™. Total of 66 samples were collected in scenario 3.

In scenario 4, Concorde Cell™ was again turned on and circuit was stabilized before samples were collected. Feed for the Concorde Cell™ was changed to NC3T to compare effects of Concorde Cell™ with different feed. Total of 78 samples were collected.

Table 2: Collected samples in the sampling campaign.

Sample	Sample code	Only Scenarios 1&4
Flotation feed	MFF	
Copper Final Concentrate	CFC	
Copper Scavenger Tail	CST	
Nickel Final Concentrate	NFC	
Nickel Flotation Tail	NI T	
Nickel Rougher Concentrate	NRC	
Nickel Rougher Tail	NRT	
Nickel Scavenger Concentrate	NSC	
Nickel Cleaner Tail	NCT	
Nickel Cleaner 4 Concentrate	NC4C	X
Nickel Cleaner 2 Concentrate	NC2C	
Nickel Cleaner 3 Tail	NC3T	
Nickel Flotation Feed	NFF	
Nickel Scavenger Feed	NSF	
Nickel Cleaner 1 Feed	NC1F	
Nickel Cleaner 1 Cells 1-2 Concentrate	NC1-1C	
Nickel Cleaner 2 Feed	NC2F	
Nickel Cleaner 2 Tail	NC2T	
Nickel Cleaner 3 Feed	NC3F	
Nickel Cleaner 3 Concentrate	NC3C	
Nickel Cleaner 4 Tail	NC4T	
Nickel Cleaner 1 Cells 1-2 Tail	NC1-1T	
Nickel Cleaner 1 Cells 3-6 Concentrate	NC1-2C	
Concorde Cell™ Feed	NCNF	X
Concorde Cell™ Concentrate	NCNC	X
Concorde Cell™ Tail	NCNT	X

Process flowsheet for each scenario and sample locations are presented in figures 17, 18 and 19.

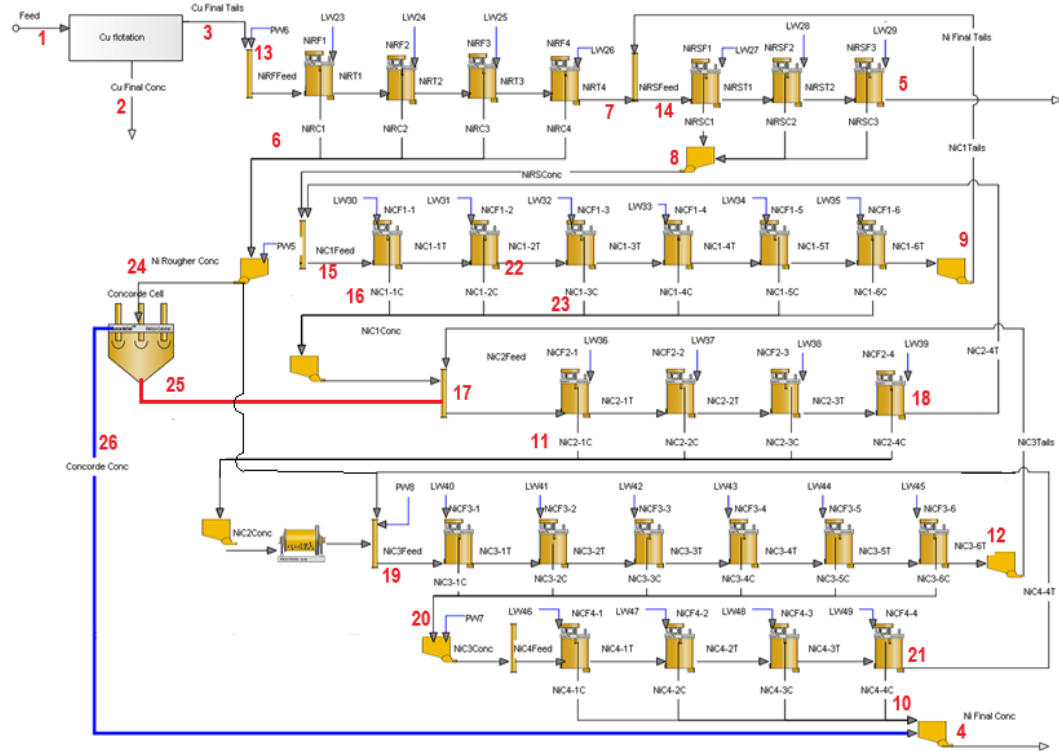


Figure 17. Nickel circuit flow sheet and sample points for scenario 1 with NRC fed into the Concorde Cell™.

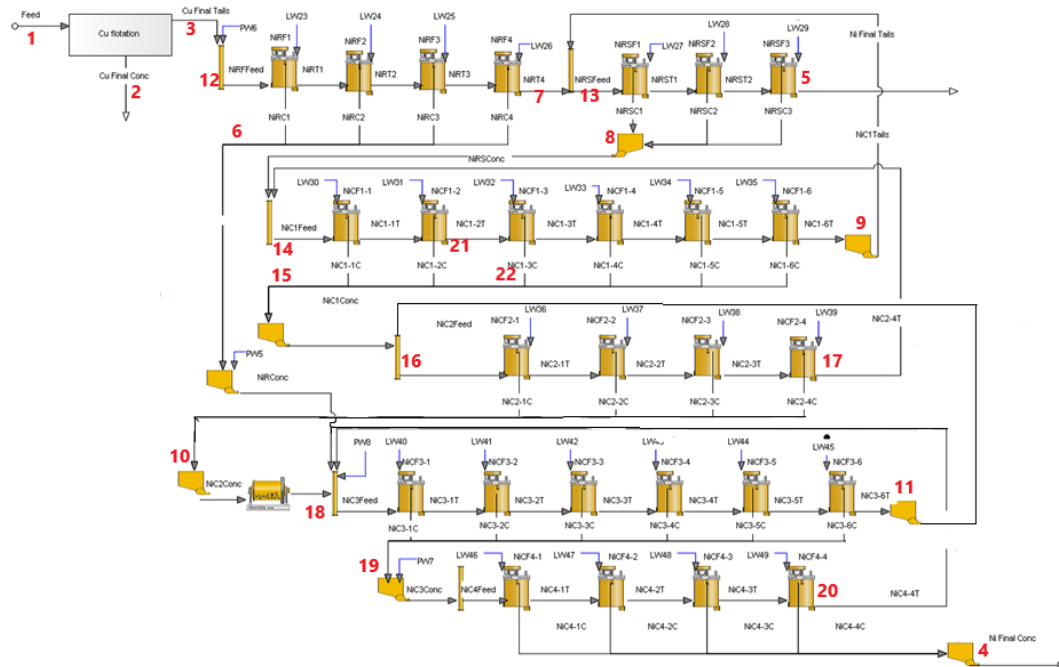


Figure 18. Nickel circuit flowsheet and sample points for baseline sampling for scenario 2 & 3.

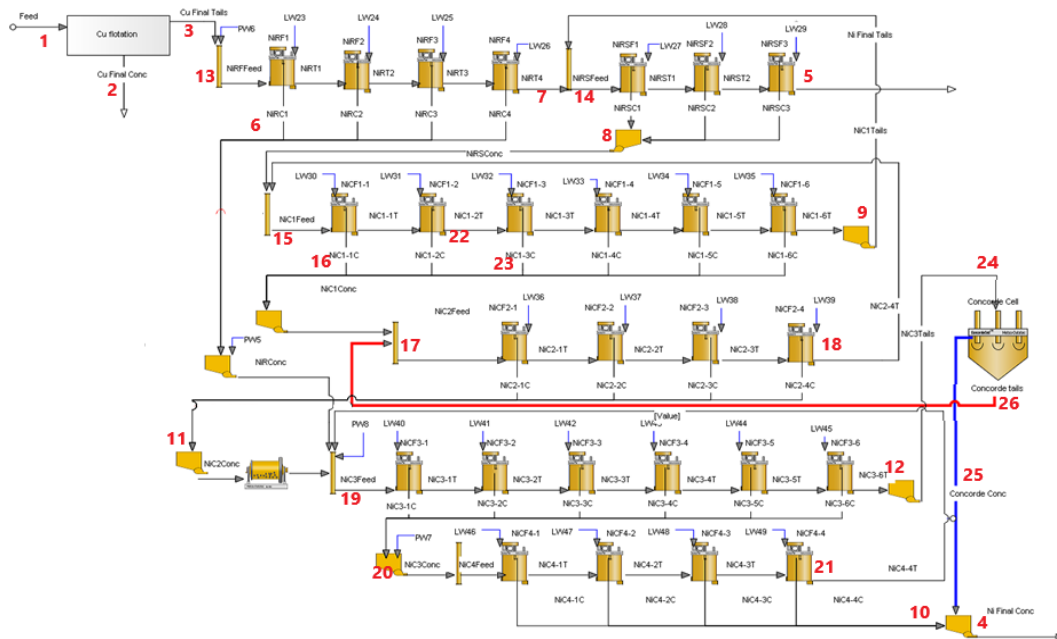


Figure 19. Nickel circuit flowsheet and sample points for scenario 4 with NC3T fed into the Concorde Cell™.

3.2.3 Mass balancing

Assays and densities were used to produce a mass balanced chart of the nickel circuits performance with and without the Concorde Cell™. For mass balancing HSC Chemistry 10 software by Metso was used. HSC Chemistry 10 is a software for process modelling. It is widely used in metallurgical industry for research, process design and development. It consists of several different modules for different uses. There are modules for process simulation, reaction equations, life cycle assessment, mass balance, diagrams and it has a vast database of elements, chemicals and minerals. For this sampling campaign, mass balancing module was used. (*HSC Chemistry*, n.d.) HSC mass balancing module can be used to estimate the performance of the process or to detect bottlenecks of the circuit. (*Mass Balancing Module*, n.d.) A model of kevitsa mill flotation circuit was constructed into mass balancing module. In the model, copper flotation was treated as a single block consisting of flotation

feed, copper final concentrate and copper tails. For nickel flotation circuit all flotation cells and streams were constructed. Model ends with the nickel tails; sulphur flotation was not considered.

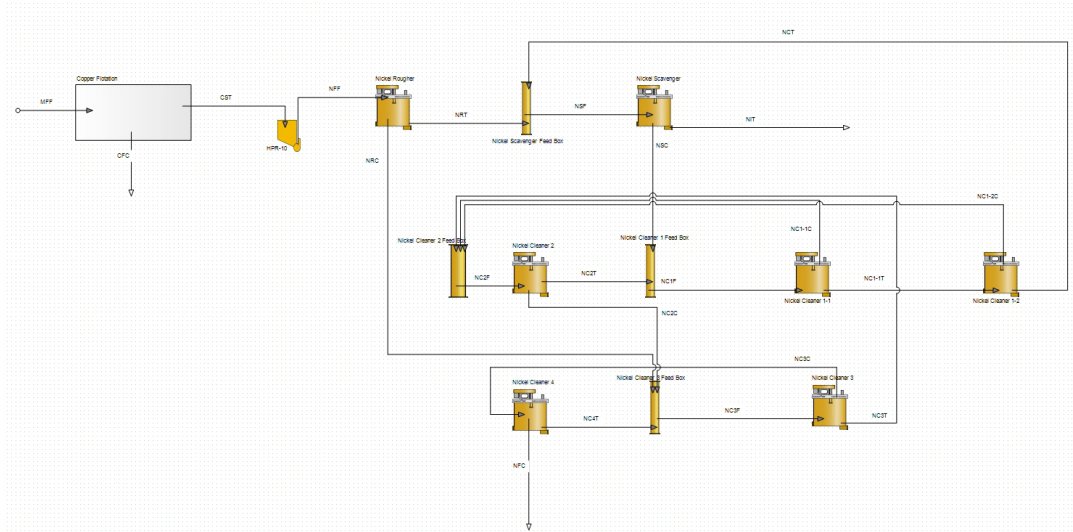


Figure 20. Flowsheet for scenarios 2 & 3 in HSC Chemistry 10.

3.3 Recovery by size

For recovery by size analysis, samples from sampling campaign were used. Samples were screened into 3 fractions: <math> < 25\mu\text{m}</math>, $25\text{-}106\mu\text{m}$ and $> 106\mu\text{m}$. For under $25\mu\text{m}$ fraction wet screening with a $25\mu\text{m}$ screen was used. For other fractions dry screening was done and $25\mu\text{m}$ and $106\mu\text{m}$ screen was used. All fractions were weighed and sent to Eurofins Labtium Oy for chemical analysis. To produce mass balanced recoveries for metals in size fractions Metso HSC10 mass balancing module was used.

4 Results

4.1 Scenario 1

4.1.1 Mill stability in scenario 1

In scenario 1 flotation feed remained stable during the sampling period. Dry feed was 1258 tons per hour on average and slurry feed volume was 2406 m³/h at 39,9% density on average. Samples were collected between 7AM and 3PM. Feed measurements during the day are shown in figure 21.

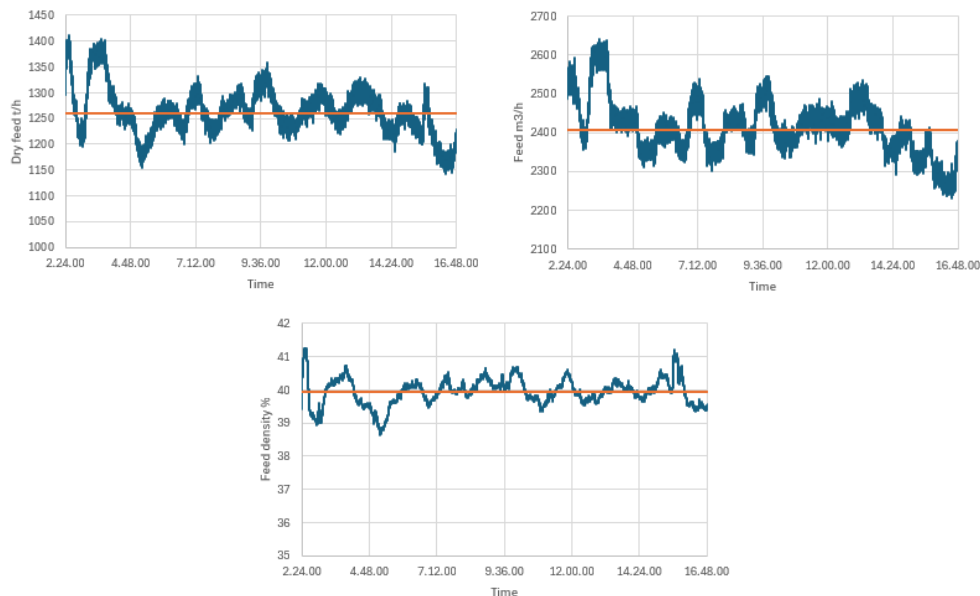


Figure 21. Mill stability in scenario 1.

4.1.2 Scenario 1 results

In scenario 1 flotation circuit recovered 82,2% of copper-to-copper concentrate and 65,1% of nickel-to-nickel concentrate. In scenario 1 Concorde was on and NRC was fed to the cell. Results from mass balanced assays are shown in table 3.

Table 3: Grades and recoveries in scenario 1.

	Flotation Feed	Copper Concentrate	Nickel Concentrate	Concorde Cell™
Ni Grade %	0,2371	0,651	11,27	11,33

Cu Grade %	0,2310	18,83	1,098	1,036
Ni Recovery %	100	2,766	65,1	33,7
Cu Recovery %	100	82,2	6,24	3,17
Mass Flow t/h	1272	12,82	16,69	8,98

In scenario 1 Concorde Cell™ accounted for 33,65% of nickel recovery, with NC4C accounting for 28,69%.

4.2 Scenario 2

4.2.1 Mill stability in scenario 2

In scenario 2 flotation feed remained relatively stable. After 9AM conveyor feeding one of the mills was stopped due to problems with the conveyor which resulted in a drop in dry flotation feed and flotation feed volumes. Samples were collected between 7AM and 3PM. No samples were gathered during the drop in flotation feed. In average dry flotation feed was 1203 tons per hour and flotation feed volume was 2358 m³/h with 39,2% density. Flotation feed measured during the day is shown in figure 22.

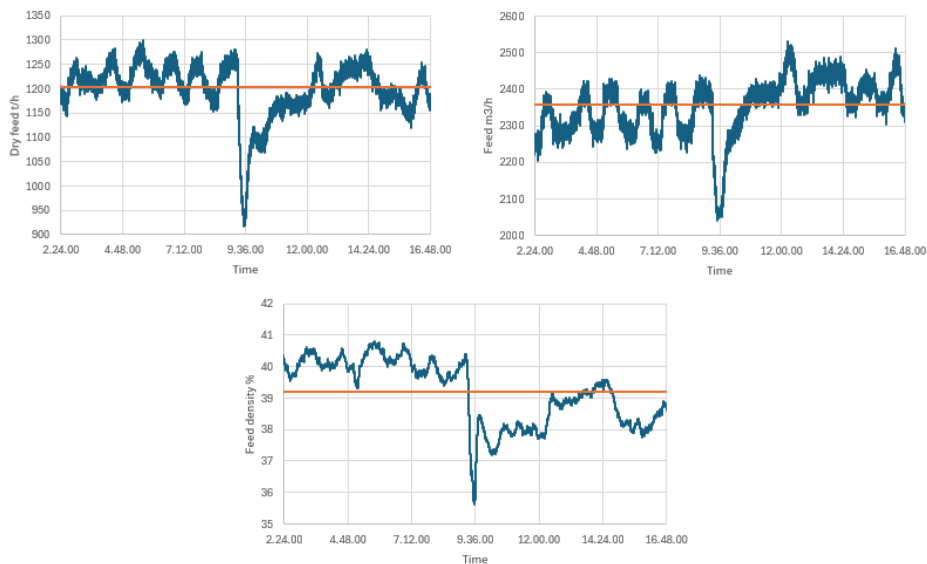


Figure 22. Mill stability in scenario 2.

4.2.2 Scenario 2 results

With scenario 2 flotation circuit recovered 82,4% of copper-to-copper concentrate and 61,4% nickel to nickel concentrate. In scenario 2 concorde was off. Mass balanced assays are represented in table 4.

Table 4: Grades and recoveries in scenario 2.

	Flotation Feed	Copper Concentrate	Nickel Concentrate	Concorde Cell™
Ni Grade %	0,2234	0,777	9,96	
Cu Grade %	0,2320	21,35	1,026	
Ni Recovery %	100	3,115	61,4	
Cu Recovery %	100	82,4	6,09	
Mass Flow t/h	1215	10,88	16,74	

4.3 Scenario 3

4.3.1 Mill stability in scenario 3

In scenario 3 mill feed remained stable during sampling. Dry flotation feed was on average 1218 tons per hour and flotation feed volume was 2324 m³/h with 40% density. Samples were collected between 7AM and 3PM. Flotation feed measurements for scenario 3 is shown in figure 23.

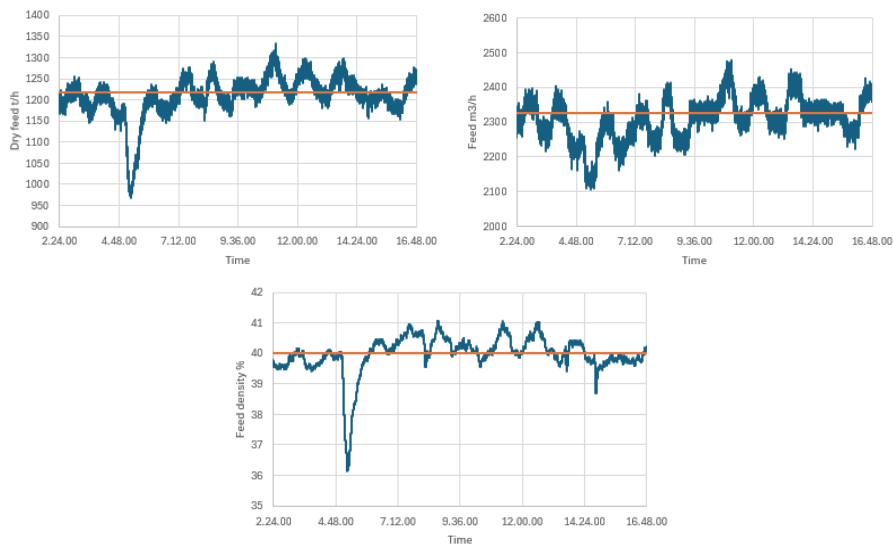


Figure 23. Mill stability in scenario 3.

4.3.2 Scenario 3 results

With scenario 3 flotation circuit recovered 80,4% of copper-to-copper concentrate and 64,7% of nickel-to-nickel circuit. In scenario 3 concorde was off. Mass balanced assays are shown in table 5.

Table 5: Grades and recoveries in scenario 3.

	Flotation Feed	Copper Concentrate	Nickel Concentrate	Concorde Cell™
Ni Grade %	0,2561	0,876	10,84	
Cu Grade %	0,2266	21,37	0,975	
Ni Recovery %	100	2,917	64,7	
Cu Recovery %	100	80,4	6,58	
Mass Flow t/h	1230	10,49	18,81	

4.4 Scenario 4

4.4.1 Mill stability in scenario 4

With scenario 4 mill feed remained stable during the sampling period. Dry flotation feed was on average 1235 tons per hour and flotation feed volume was 2385 m³/h with 39,6% density. Samples were collected between 7AM and 12:30PM. After sampling was conducted, due to problems in milling, all mills had to be shutdown, this did not affect the sampling since all samples were already gathered. Averages of the feed were calculated from the time during the sampling before the shutdown.

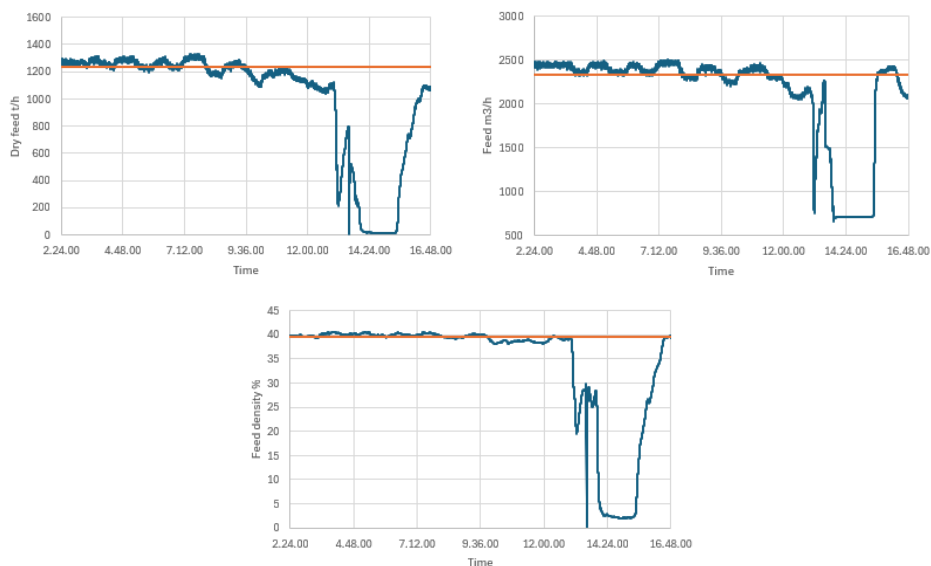


Figure 24. Mill stability in scenario 4.

4.4.2 Scenario 4 results

In scenario 4 flotation circuit recovered 82,7% of copper-to-copper concentrate and 63,4 nickel to nickel concentrate. In scenario 4 Concorde was on and NC3T was fed to the cell. Mass balanced assays are shown in table 6.

Table 6: Grades and recoveries in scenario 4.

	Flotation Feed	Copper Concentrate	Nickel Concentrate	Concorde Cell™
Ni Grade %	0,2021	0,803	11,22	4,94
Cu Grade %	0,2295	21,29	1,090	0,390
Ni Recovery %	100	3,54	63,4	3,51
Cu Recovery %	100	82,7	5,42	0,2440
Mass Flow t/h	1247	11,12	14,23	1,789

In scenario 4 Concorde Cell™ only accounted for 3,51% of the nickel recovery while NC4C accounted for 59,85%.

4.5 Size by size recovery

4.5.1 Scenario 1

From scenario 1, round 1 was chosen to be screened. In scenario 1 Concorde was on and NRC was fed to the cell.

Table 7: Mass balancing results from scenario 1 screening.

	MFF Ni-Grade	MFF weight retained	NFC Ni-Grade	NFC Ni-Recovery	NFC weight retained
Bulk	0,2017	100	8,71	57,0	100
0,212-0,106mm	0,0991	18,31	5,03	38,2	10,46
0,106-0,025mm	0,2003	38,9	9,92	67,0	39,8
0,025-0mm	0,2470	42,8	8,50	52,8	49,7

Table 8: Mass balancing results from Concorde Cell™ screening in scenario 1.

	NCNF Ni Grade	NCNF Weight	NCNC Ni Grade	NCNC Ni Recovery	NCNC Weight
Bulk	4,40	100	9,93	65,5	100
0,212-0,106mm	0,80	3,4	1,51	65,7	4,1
0,106-0,025mm	6,61	23,19	10,71	75,6	37,3
0,025-0mm	3,860	73,4	10,03	60,1	58,6

In scenario 1 NRC was fed to the Concorde Cell™. Concorde Cell™ alone was able to produce 16,5% better grade concentrate than the total circuit. In fine particles under the size of 25 microns Concorde Cell™ was able to recover 60% of the nickel and it had better recoveries in all particle sizes compared to the total circuit. Poorest nickel grade was in the coarse fraction of the feed and poorest recovery of nickel-to-nickel concentrate was in the coarse fraction.

4.5.2 Scenario 2

From scenario 2 round 4 was selected for screening. In scenario 2 concorde was off.

Table 9: Mass balancing results from scenario 2 screening.

	MFF Ni-Grade	MFF weight retained	NFC Ni-Grade	NFC Ni-Recovery	NFC weight retained
Bulk	0,2309	100	11,34	61,2	100
0,212-0,106mm	0,0872	13,04	5,95	26,88	4,12
0,106-0,025mm	0,2112	38,5	11,43	74,5	42,5
0,025-0mm	0,2852	48,4	11,67	56,3	53,4

Nickel recovery was at a traditional level at 61,5 % percent with the highest recoveries again being at the coarse and especially middle size fraction.

Poorest recovery of nickel-to-nickel concentrate performance was again in the fine fraction.

4.5.3 Scenario 3

In scenario 3 round 8 was selected for screening. In scenario 3 concorde was off.

Table 10: Mass balancing results from scenario 3 screening.

	MFF Ni-Grade	MFF weight retained	NFC Ni-Grade	NFC Ni-Recovery	NFC weight retained
Bulk	0,2618	100	10,78	64,7	100
0,212-0,106mm	0,0944	4,72	0,754	39,3	14,79
0,106-0,025mm	0,2257	38,9	11,46	77,2	37,6
0,025-0mm	0,3007	56,4	13,35	58,9	47,6

For scenario 3 nickel grade in the feed was higher in all fractions than in scenario 2. Nickel recovery was also improved in all fractions. Fine fraction nickel grade was over 13% and fine fraction accounted for over 47% of the total nickel concentrate by weight.

4.5.4 Scenario 4

In scenario 4 round 12 was chosen for screening. In scenario 4 Concorde was on and NC3T was fed in to the cell.

Table 11: Mass balancing results from scenario 4 screening.

	MFF Ni-Grade	MFF weight retained	NFC Ni-Grade	NFC Ni-Recovery	NFC weight retained
Bulk	0,1983	100	10,74	63,8	100
0,212-0,106mm	0,0665	14,12	4,92	29,95	4,84
0,106-0,025mm	0,1883	39,1	10,84	77,9	44,8
0,025-0mm	0,2465	46,8	11,2	57,7	50,3

Table 12: Mass balancing results from the Concorde Cell™ screening in scenario 4.

	NCNF Ni Grade	NCNF Weight	NCNC Ni Grade	NCNC Ni Recovery	NCNC Weight
Bulk	2,47	100	4,67	32,6	100
0,212-0,106mm	0,69	2,0	0,86	26,0	2,4
0,106-0,025mm	1,16	27,53	2,64	52,6	37,0
0,025-0mm	3,034	70,4	6,07	29,7	60,6

In scenario 4 NC3T was fed into the Concorde Cell™. The cell was able to produce around 4% nickel concentrate. Fine particle size nickel recovery was 60,6% which was significantly better than the 29,94% nickel recovery by the total circuit. Medium size nickel recovery was also higher at 66,2%.

4.6 Summary

4.6.1 Flotation circuit stability

Mass balanced assays and mass flow for flotation feed for scenarios 1-4 is shown in table 13.

Table 13: Flotation feed assay for nickel and copper and dry mass flow for each scenario. 1: Concorde on, NRC as feed, 2: Concorde off, 3: Concorde off, 4: Concorde on, NC3T as feed.

MFF	1	2	3	4
Ni Grade	0,2371	0,2234	0,2561	0,2021
Cu Grade	0,2310	0,2320	0,2266	0,2295
Mass Flow	1272	1215	1230	1247

Even though ore feed was kept the same throughout the sampling period, nickel grade in the feed varied significantly. In scenario 3 nickel grade was 0,26%, much higher than in scenario 4 which was 0,2021. This has the possibility to influence the nickel circuit operations and recovery dramatically. Other parameters in the feed like dry mass and density were stable throughout the sampling period. Copper grade in the feed remained stable in all scenarios.

4.6.2 Survey results summary

Mass balanced assays for scenarios 1-4 for CFC are shown in table 14.

Table 14: Copper concentrate bulk assays, recoveries and dry mass flow in each scenario.

CFC	1	2	3	4
Ni Grade	0,651	0,777	0,876	0,803
Cu Grade	18,83	21,35	21,37	21,29
Ni Recovery	2,766	3,115	2,917	3,54
Cu Recovery	82,2	82,4	80,4	82,7
Mass Flow	12,82	10,88	10,49	11,12

Copper circuit performed efficiently as it has been previously before the sampling. Scenario 1 produced more concentrate by mass which may explain

lower copper grades than the other three scenarios. Scenarios 2, 3 and 4 showed similar performance.

Mass balanced assays for scenarios 1-4 for NFC are shown in table 15.

Table 15: Nickel concentrate assays, recoveries and dry mass flow in each scenario.

NFC	1	2	3	4
Ni Grade	11,27	9,96	10,84	11,22
Cu Grade	1,098	1,026	0,975	1,090
Ni Recovery	62,3	61,4	64,7	63,4
Cu Recovery	6,24	6,09	6,58	5,42
Mass Flow	16,69	16,74	18,81	14,23

Nickel circuit copper grade was around 1% for all scenarios. Scenario 1 and 2 produced similar amount of concentrate by mass. With Concorde Cell™ in use at scenario 1 grade was 11,27%, better than in baseline scenario 2 at 9,96%. Nickel recovery in scenario 1 was also better than in scenario 2. With Concorde Cell™ in use in scenario 4 nickel grade was again better than in baseline scenario 3. Nickel recovery was lower in scenario 4 than in baseline scenario 3. Scenario 4 produced 25% less concentrate by mass than scenario 3, which may result from less mass pull resulting in lower recovery and better overall grade.

Recovery of nickel to tailings is shown in table 16.

Table 16: Recovery of nickel to tailings.

	1	2	3	4
NRT	32,1	32,4	40,4	38,5
NCT	11,65	7,07	17,35	11,92
NiT	34,9	35,5	32,4	33,1

Nickel grade in nickel rougher tailings and nickel cleaner tailings were highest in scenario 3, where also the nickel grade in feed was the highest. In other scenarios nickel cleaner tailings nickel grade were between 7% and 12%. Nickel grade in nickel final tailings were above 30% for all scenarios.

4.6.3 Size-by-size results summary

Screened analysis of the MFF samples is shown in table 16.

Table 17: Size-by-size assays of flotation feed in each scenario.

MFF Grades	1	2	3	4
Bulk	0,2017	0,2309	0,2618	0,1983
0,212-0,106mm	0,0991	0,0872	0,0944	0,0665
0,106-0,025mm	0,2003	0,2112	0,2257	0,1883
0,025-0mm	0,2470	0,2852	0,3007	0,2465

Overall nickel grades in feed varied between 0,1983% and 0,2618% with scenario 4 being the lowest grade and scenario 3 being the highest in grade. In fine particles between 0,0 and 0,025mm grades were constantly higher than the bulk sample, with scenario 4 being the lowest and scenario 3 being the highest of grade, making comparisons between scenarios 3 & 4 difficult. Medium size particles from 0,106 to 0,025mm varied less than the coarse particles. With coarse particles, more than 0,106mm in size, scenario 1 contained the most nickel 0,0991% and scenario 4 contained again the least nickel at 0,0665%.

Particle size distribution by weight is shown in table 18.

Table 18: Particle size distribution of flotation feed in each scenario.

MFF by weight	1	2	3	4
Bulk	100	100	100	100
0,212-0,106mm	18,31	13,04	4,72	14,12
0,106-0,025mm	38,9	38,5	38,9	39,1
0,025-0mm	42,8	48,4	56,4	46,8

Particle size distribution in feed was quite constant with fine and medium size particles. Largest variation was with round 3 which had only 4,72% of coarse particles which may be result of fine grinding or from screening and assay error. Size-by-size analysis was done for one round per scenario, which increases the risk for errors in sampling and sample preparation. Sampling takes place only for some seconds and process disturbances may occur just when sample is being taken. No major process disturbances were detected in milling or flotation feed during sampling.

NFC assays by size are shown in table 19.

Table 19: Size-by-size assays of nickel concentrate in each scenario.

NFC Grades	1	2	3	4
Bulk	8,71	11,34	10,78	10,74
0,212–0,106mm	5,03	5,95	0,754	4,92
0,106–0,025mm	9,92	11,43	11,46	10,84
0,025-0mm	8,50	11,67	13,35	11,2

In scenario 1 bulk, fine and medium size fractions contained less nickel than other scenarios. In scenario 3 coarse particles contained only 0,754% of nickel most likely due to small number of fine particles in the feed or errors mentioned previously.

Nickel recovery to NFC by scenario is shown in table 20.

Table 20: Nickel recoveries by size in each scenario.

NFC Recoveries	1	2	3	4
Bulk	57,0	61,2	64,7	63,8
0,212–0,106mm	38,2	26,88	39,3	29,95
0,106–0,025mm	67,0	74,5	77,2	77,9
0,025-0mm	52,8	56,3	58,9	57,7

Overall nickel recovery to nickel concentrate was in a traditional level. Scenario 1 recovery was the lowest at 57% and highest recovery was achieved in scenario 3 at 64,7%. Fine nickel recovery was highest in scenario 3 when Concorde Cell™ was not in use at 59%. In scenario 4 fine nickel recovery was 58%, highest when Concorde Cell™ was in operation. Size-by-size nickel recoveries were made for single rounds due to workload and since vary slightly from plant mass balances which were made with three round averages.

NFC particle size distribution by sample is shown in table 21.

Table 21: Particle size distribution in nickel concentrate in each scenario.

NFC by weight	1	2	3	4
Bulk	100	100	100	100
0,212-0,106mm	10,46	4,12	14,79	4,84
0,106-0,025mm	39,8	42,5	37,6	44,8
0,025-0mm	49,7	53,4	47,6	50,3

Particle size distribution was constant for NFC in medium particles. Fine particles recovery was highest in scenario 2 with 53,4% and lowest in scenario 3 with 47,6%. Coarse particle recovery varied significantly with round 3 being the highest at 14,79% and lowest in scenario 2 with 4,12%.

5 Conclusions

Purpose of this study was to investigate the effects of the Concorde Cell™ to the Kevitsa mill flotation circuit. This was done with a sampling campaign for four days to produce mass balanced results of the flotation circuit behaviour with and without the Concorde Cell™.

Feed significantly influences the overall performance of the circuit. Even though ore feed was kept the same throughout the sampling period, nickel grades in the ore finger changed by almost 27%. This makes comparisons between scenarios more difficult. In scenario 4 also higher grade and lower production of concentrate by mass indicates that the circuit was operated with less mass pull leading to lower recoveries and higher concentrate grade.

Nickel rougher recovery was for scenarios 1 and 2 similar to the total nickel recovery of the circuit. Nickel scavenger recovery for scenarios 1 and 2 was less than 9% indicating a small impact to the overall recovery of the circuit. Around 10% of the nickel was lost to the cleaner circuit tailings while nickel circuit final tailings were around 30-35%. Nickel rougher tailings were already around 32%. This suggests that nickel cleaner circuit operates quite efficiently. Comparing scenarios 3 and 4, without Concorde Cell™ in scenario 3 nickel cleaner tailings were over 17% while with the Concorde Cell™ in scenario 4 nickel cleaner tailings was only under 12% indicating that Concorde Cell™ together with the cleaner circuit was able to recover more of the nickel circulating in the cleaner circuit.

Due to the size of the Concorde Cell™ it limits the amount of fresh feed it can take. Currently only around half of the total slurry stream was fed into the Concorde Cell™. This could also influence the effects of the cell and make the effects less noticeable. Concorde Cell™ itself indicated good performance. The cell was able to recover almost 60% of fine nickel under 25microns from the nickel rougher concentrate and almost 30% of fine nickel from the nickel cleaner 3 tailings. In scenario 1 while Concorde Cell™ was fed with

NRC, the cell was able to improve overall nickel recovery by 1,5% compared to scenario 2 without the Concorde Cell™. In scenario 4 even with significantly lower nickel feed than in scenario 3, the recovery was good both overall and in fines.

When nickel rougher concentrate was fed into the Concorde Cell™ the cell produced significantly higher-grade concentrates than with nickel cleaner 3 tailings as feed and accounted for 33,65% nickel recovery compared to 3,51% nickel recovery in scenario 4. This suggests that rougher concentrate is by far more floatable material than the material in nickel cleaner 3 tailings. Since Concorde Cell™ operates in the cleaning circuit of the mill, material in the feed and circulation could already be too oxidized that even the Concorde Cell™ is not able to recover these particles.

Since the overall nickel concentrate nickel grade target is around 8-10%, Concorde Cell™ can help the total nickel circuit if it is not able to produce high enough grade, since it can produce over 10% nickel grades at least from the nickel rougher concentrate stream. If the nickel circuit can produce high enough grade concentrates Concorde Cell™ should be operated with maximum feed and maximum mass pull in order to keep the recovery of nickel as high as possible.

Froth stability should also be considered in more detail when looking at the effects of the Concorde Cell™. The cell is removing fine particles from the cleaner circuit which could influence the froth stability.

More research should be done to the nickel rougher-scavenger circuit to see if it could recover more nickel in the early stages of the process before particles are not floatable. Having more flotation capacity in the nickel cleaner circuit could allow the nickel rougher and nickel scavenger circuits to pull more nickel to the cleaner circuit. Since the Concorde Cell™ currently is only operating with part of a stream its effects could be difficult to notice.

Having additional Concorde Cell™ would allow whole streams to be floated with the Concorde Cell™. This should lead to more noticeable effects in the nickel circuit. The Concorde Cell™ was able to produce high-grade concentrate with high recoveries, which indicates that additional cells should have positive effects to the circuit.

More size-by-size comparison surveys should be done to have more data with similar feed grades for more accurate comparisons about the circuit performance with and without the Concorde Cell™.

References

- Bulatovic, S. M. (2007). *Handbook of flotation reagents: Chemistry, theory and practice. Vol. 1: Flotation of sulphide ores* (Vol. 1). Elsevier.
- Calvo, G., Mudd, G., Valero, A., & Valero, A. (2016). Decreasing Ore Grades in Global Metallic Mining: A Theoretical Issue or a Global Reality? *Resources*, 5(4), 4. <https://doi.org/10.3390/resources5040036>
- Chen, J., Chimonyo, W., & Peng, Y. (2022). Flotation behaviour in reflux flotation cell – A critical review. *Minerals Engineering*, 181, 107519. <https://doi.org/10.1016/j.mineng.2022.107519>
- Farrokhpay, S., Filippov, L., & Fornasiero, D. (2021). Flotation of Fine Particles: A Review. *Mineral Processing and Extractive Metallurgy Review*, 42(7), 473–483. <https://doi.org/10.1080/08827508.2020.1793140>
- Fuerstenau, M. C., Jameson, G. J., & Yoon, R.-H. (Eds.). (2009). *Froth flotation: A century of innovation*. Society for Mining, Metallurgy, and Exploration.
- Han, S., Jung, M., Lee, W., Kim, S., Lee, K., Lim, G., Jeon, H.-S., Choi, S. Q., & Han, Y. (2021). Diagnosis and Optimization of Gold Ore Flotation Circuit via Linear Circuit Analysis and Mass Balance Simulation. *Minerals*, 11(10), 1065. <https://doi.org/10.3390/min11101065>
- Hanumantha Rao, K., & Forssberg, K. S. E. (1997). Mixed collector systems in flotation. *International Journal of Mineral Processing*, 51(1), 67–79. [https://doi.org/10.1016/S0301-7516\(97\)00039-2](https://doi.org/10.1016/S0301-7516(97)00039-2)
- Harbort, G., De Bono, S., Carr, D., & Lawson, V. (2003). Jameson Cell fundamentals—a revised perspective. *Minerals Engineering*, 16(11), 1091–1101. <https://doi.org/10.1016/j.mineng.2003.06.008>
- HSC Chemistry. (n.d.). Metso. Retrieved 1 April 2025, from <https://www.metso.com/portfolio/hsc-chemistry/>

- Jameson, G. J. (2010a). Advances in Fine and Coarse Particle Flotation. *Canadian Metallurgical Quarterly*, 49(4), 325–330.
<https://doi.org/10.1179/cmq.2010.49.4.325>
- Jameson, G. J. (2010b). New directions in flotation machine design. *Minerals Engineering*, 23(11), 835–841. <https://doi.org/10.1016/j.mineng.2010.04.001>
- Liu, T. Y., & Schwarz, M. P. (2009). CFD-based modelling of bubble-particle collision efficiency with mobile bubble surface in a turbulent environment. *International Journal of Mineral Processing*, 90(1), 45–55.
<https://doi.org/10.1016/j.minpro.2008.10.004>
- Mass Balancing Module. (n.d.). Metso. Retrieved 1 April 2025, from <https://www.metso.com/portfolio/hsc-chemistry/mass-balancing-module/>
- Mesa, D., & Brito-Parada, P. R. (2019). Scale-up in froth flotation: A state-of-the-art review. *Separation and Purification Technology*, 210, 950–962.
<https://doi.org/10.1016/j.seppur.2018.08.076>
- Miettinen, T., Ralston, J., & Fornasiero, D. (2010). The limits of fine particle flotation. *Minerals Engineering*, 23(5), 420–437.
<https://doi.org/10.1016/j.mineng.2009.12.006>
- Musuku, B. (2024). *A Methodology for Systemic Plant Research: An Industrial Case Study Investigating the Effects of Water Quality on Pentlandite Flotation Recovery*. Aalto University. <https://aaltodoc.aalto.fi/handle/123456789/126842>
- Neethling, S. J., & Cilliers, J. J. (2012). Grade-recovery curves: A new approach for analysis of and predicting from plant data. *Minerals Engineering*, 36–38, 105–110. <https://doi.org/10.1016/j.mineng.2012.02.018>

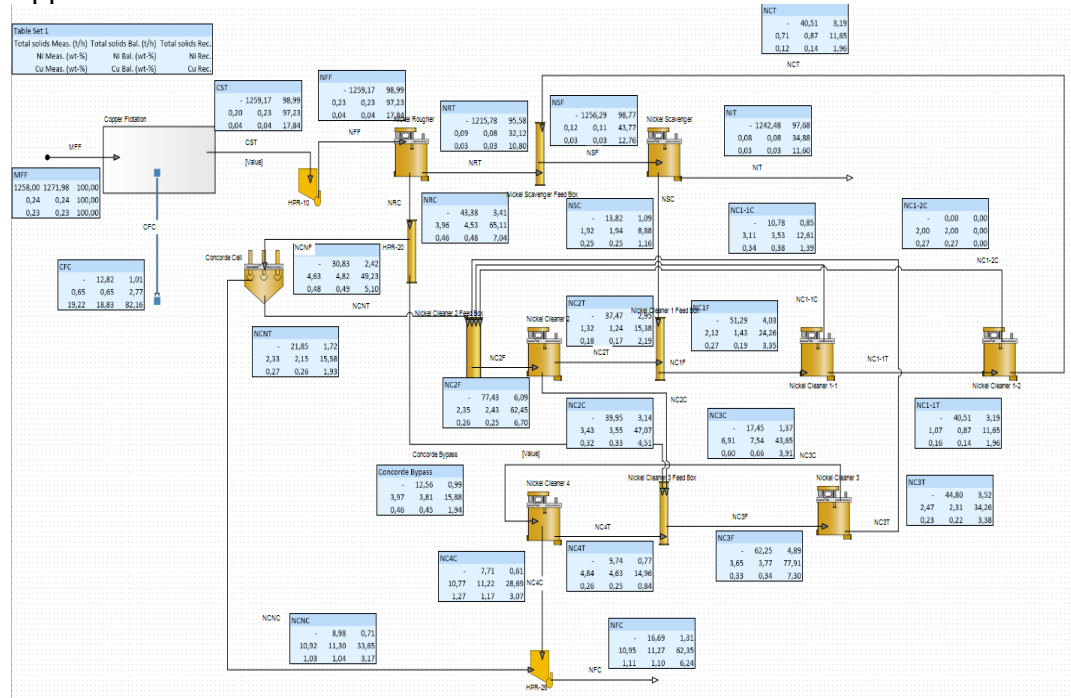
- Norori-McCormac, A., Brito-Parada, P. R., Hadler, K., Cole, K., & Cilliers, J. J. (2017). The effect of particle size distribution on froth stability in flotation. *Separation and Purification Technology*, 184, 240–247. <https://doi.org/10.1016/j.seppur.2017.04.022>
- Pease, J. D., Curry, D. C., & Young, M. F. (2006). Designing flotation circuits for high fines recovery. *Minerals Engineering*, 19(6), 831–840. <https://doi.org/10.1016/j.mineng.2005.09.056>
- Prakash, R., Majumder, S. K., & Singh, A. (2018). Flotation technique: Its mechanisms and design parameters. *Chemical Engineering and Processing - Process Intensification*, 127, 249–270. <https://doi.org/10.1016/j.cep.2018.03.029>
- Somasundaran, P., & Wang, D. (Eds.). (2006). *Solution chemistry: Minerals and reagents* (1st ed). Elsevier.
- Tao, D. (2005). Role of Bubble Size in Flotation of Coarse and Fine Particles—A Review. *Separation Science and Technology*, 39(4), 741–760. <https://doi.org/10.1081/SS-120028444>
- Wills, B. A., & Finch, J. E. (2016). *Wills' mineral processing technology: An introduction to the practical aspects of ore treatment and mineral recovery* (Eighth edition). Elsevier.
- Wills, B. A., & Napier-Munn, T. (2006). *Wills' Mineral Processing Technology: An Introduction to the Practical Aspects of Ore Treatment and Mineral Recovery*. Elsevier Science & Technology. <http://ebookcentral.proquest.com/lib/aalto-ebooks/detail.action?docID=294444>
- Yáñez, A., Kupka, N., Tunç, B., Suhonen, J., & Rinne, A. (2024). Fine and ultrafine flotation with the Concorde Cell™™ – A journey. *Minerals Engineering*, 206, 108538. <https://doi.org/10.1016/j.mineng.2023.108538>

APPENDIX

Appendix 1. Mass balance results scenario 1.

Stream	solids t/h	NI Bal. (wt-%)	Cu Bal. (wt-%)	solids Re Cu % Meas.	Cu % Bal.	Cu Rec %	Ni % Meas.	Ni % Bal.	Ni Rec %
NSC	13,82	1,086	0,2508	0,2476	1,165	1,919	1,939	8,88	
NFF	1259	99,0	0,0403	0,0416	17,84	0,2288	0,2329	97,2	
NRT	1216	95,6	0,02997	0,02610	10,80	0,0890	0,0797	32,1	
NCT	40,5	3,19	0,1180	0,1422	1,962	0,708	0,867	11,65	
NSF	1256	98,8	0,0330	0,02984	12,76	0,1210	0,1051	43,8	
Concorde Bypass	12,56	0,987	0,460	0,454	1,941	3,97	3,81	15,88	
NC4C	7,71	0,606	1,266	1,171	3,072	10,77	11,22	28,69	
NCNC	8,98	0,706	1,034	1,036	3,17	10,92	11,30	33,7	
NC2F	77,4	6,09	0,2569	0,2542	6,70	2,353	2,432	62,4	
NRC	43,4	3,41	0,460	0,476	7,04	3,96	4,53	65,1	
NFC	16,69	1,312	1,113	1,098	6,24	10,95	11,27	62,3	
NC3T	44,8	3,52	0,2276	0,2218	3,38	2,469	2,306	34,3	
NC1-1T	40,5	3,19	0,1590	0,1422	1,962	1,069	0,867	11,65	
NC1F	51,3	4,03	0,2674	0,1919	3,35	2,118	1,427	24,26	
NC1-1C	10,78	0,847	0,342	0,378	1,388	3,107	3,53	12,61	
NC2T	37,5	2,946	0,1805	0,1713	2,185	1,319	1,238	15,38	
NC4T	9,74	0,766	0,2615	0,2538	0,841	4,84	4,63	14,96	
NCNT	21,85	1,718	0,2668	0,2593	1,928	2,328	2,151	15,58	
NiT	1242	97,7	0,02813	0,02742	11,60	0,0846	0,0847	34,9	
NC3F	62,3	4,89	0,335	0,344	7,30	3,65	3,77	77,9	
NC1-2C	0,0	0,0	0,2657	0,2657	0,0	2,003	2,003	0,0	
NCNF	30,83	2,423	0,476	0,486	5,10	4,63	4,82	49,2	
NC3C	17,45	1,372	0,595	0,659	3,91	6,91	7,54	43,7	
NC2C	40,0	3,141	0,325	0,332	4,51	3,43	3,55	47,1	
MFF	1258	1272	100,0	0,2290	0,2310	100,0	0,2372	0,2371	100,0
CST	1259	99,0	0,0366	0,0416	17,84	0,2047	0,2329	97,2	
CFC	12,82	1,008	19,22	18,83	82,2	0,650	0,651	2,766	

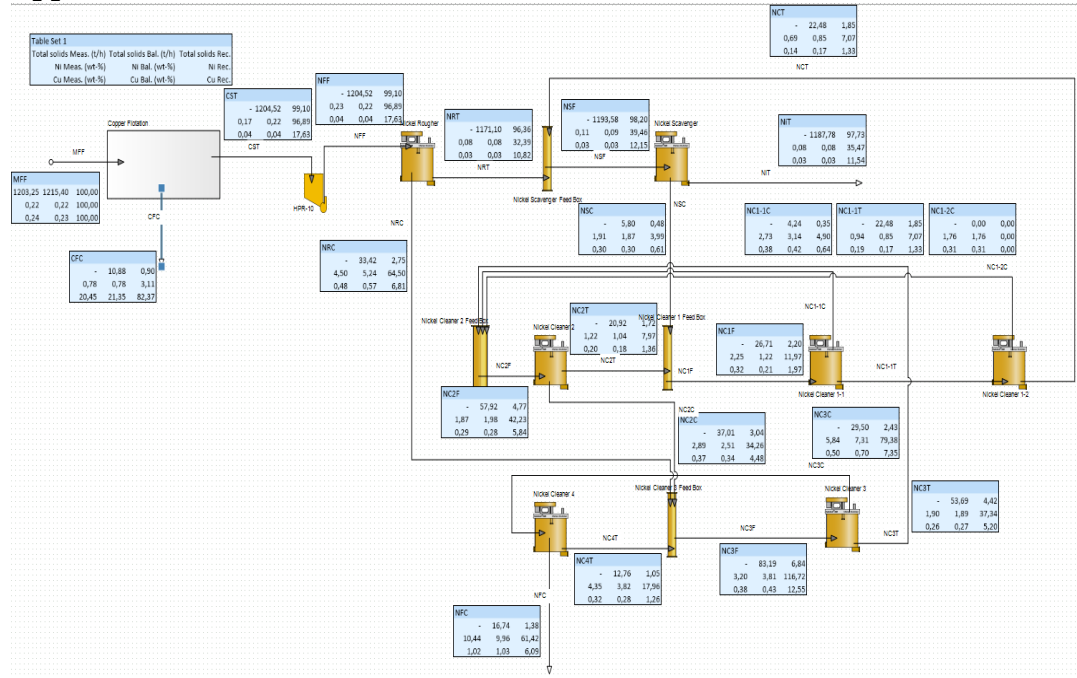
Appendix 2. Mass balanced flowsheet in scenario 1.



Appendix 3. Mass balanced results in scenario 2.

Stream	solids t/h	Nl solids t/h	al solids t/h	ReCu % Meas.	Cu % Bal.	Cu Rec %	Ni % Meas.	Ni % Bal.	Ni Rec %
CST	1203	1205	99,1	0,0384	0,0413	17,63	0,1747	0,2184	96,9
NFF	1203	1205	99,1	0,0414	0,0413	17,63	0,2252	0,2184	96,9
NRT	1203	1171	96,4	0,02867	0,02606	10,82	0,0798	0,0751	32,4
MFF	1203	1215	100,0	0,2366	0,2320	100,0	0,2232	0,2234	100,0
NCT	1203	22,48	1,849	0,1372	0,1666	1,328	0,694	0,854	7,07
NSC	1203	5,80	0,477	0,2980	0,2970	0,611	1,905	1,869	3,99
NC1-1T	1203	22,48	1,849	0,1852	0,1666	1,328	0,937	0,854	7,07
NC2F	1203	57,9	4,77	0,2858	0,2841	5,84	1,867	1,980	42,2
NC3C	1203	29,50	2,427	0,496	0,703	7,35	5,84	7,31	79,4
NFC	1203	16,74	1,377	1,021	1,026	6,09	10,44	9,96	61,4
NC3F	1203	83,2	6,84	0,382	0,425	12,55	3,20	3,81	116,7
NC4T	1203	12,76	1,050	0,322	0,2793	1,264	4,35	3,82	17,96
NiT	1203	1188	97,7	0,02717	0,02739	11,54	0,0812	0,0811	35,5
NC3T	1203	53,7	4,42	0,2634	0,2730	5,20	1,900	1,888	37,3
NSF	1203	1194	98,2	0,0320	0,02870	12,15	0,1062	0,0898	39,5
NC2T	1203	20,92	1,721	0,2045	0,1828	1,356	1,217	1,035	7,97
CFC	1203	10,88	0,895	20,45	21,35	82,4	0,781	0,777	3,115
NC1-1C	1203	4,24	0,349	0,384	0,425	0,638	2,728	3,137	4,90
NC2C	1203	37,0	3,045	0,371	0,341	4,48	2,888	2,514	34,3
NC1-2C	1203	0,0	0,0	0,3145	0,3145	0,0	1,756	1,756	0,0
NC1F	1203	26,71	2,198	0,318	0,2076	1,966	2,247	1,216	11,97
NRC	1203	33,4	2,750	0,482	0,574	6,81	4,50	5,24	64,5

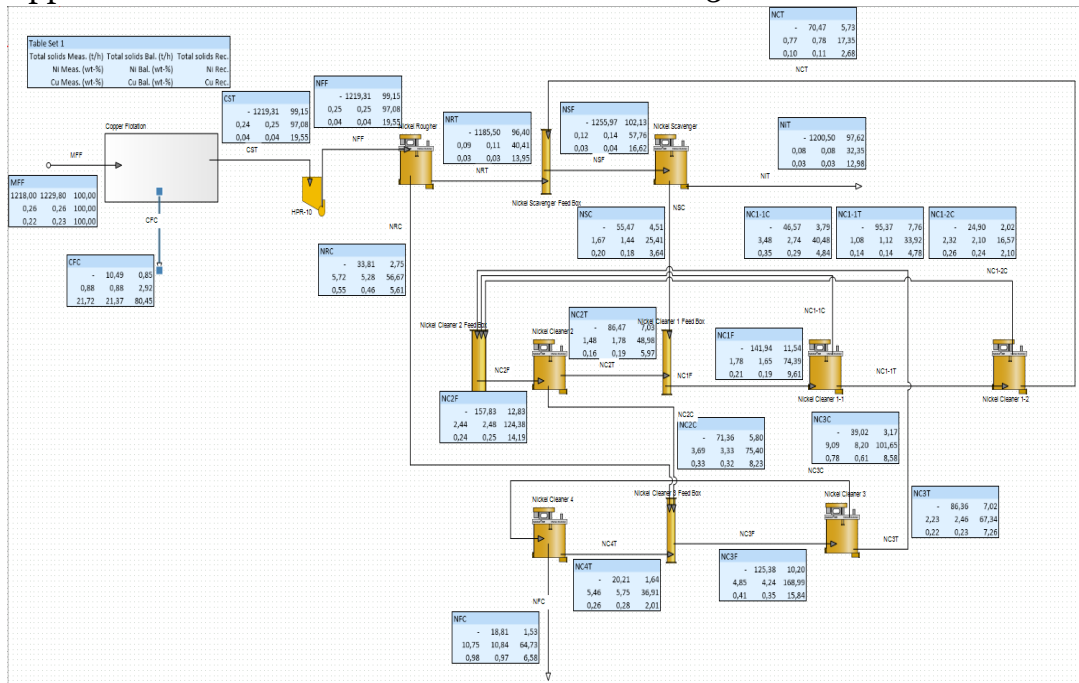
Appendix 4. Scenario 2 mass balanced flowsheet.



Appendix 5. Mass balanced results in scenario 3.

Stream	solids t/h	NI solids t/h	al solids t/h	ReCu %	Meas. Cu %	Bal. Cu %	Rec %	Meas. Ni %	Bal. Ni %	Rec %
CST	1219	99,1	0,0380	0,0447	19,55	0,2352	0,2508	97,1		
NFF	1219	99,1	0,0442	0,0447	19,55	0,2492	0,2508	97,1		
NRT	1186	96,4	0,02680	0,0328	13,95	0,0913	0,1074	40,4		
MFF	1230	100,0	0,2223	0,2266	100,0	0,2563	0,2561	100,0		
NCT	70,5	5,73	0,1038	0,1058	2,675	0,773	0,775	17,35		
NSC	55,5	4,51	0,2004	0,1831	3,64	1,666	1,443	25,41		
NC1-1T	95,4	7,76	0,1357	0,1395	4,78	1,083	1,120	33,9		
NC2F	157,8	12,83	0,2437	0,2506	14,19	2,442	2,482	124,4		
NC3C	39,0	3,17	0,778	0,613	8,58	9,09	8,20	101,6		
NFC	18,81	1,529	0,980	0,975	6,58	10,75	10,84	64,7		
NC3F	125,4	10,20	0,411	0,352	15,84	4,85	4,24	169,0		
NC4T	20,21	1,644	0,2630	0,2766	2,006	5,46	5,75	36,9		
NI T	1201	97,6	0,03047	0,03013	12,98	0,0846	0,0849	32,4		
NC3T	86,4	7,02	0,2211	0,2342	7,26	2,227	2,456	67,3		
NSF	1256	102,1	0,03007	0,0369	16,62	0,1200	0,1448	57,8		
NC2T	86,5	7,03	0,1629	0,1923	5,97	1,485	1,784	49,0		
CFC	10,49	0,853	21,72	21,37	80,4	0,875	0,876	2,917		
NC1-1C	46,6	3,79	0,350	0,2895	4,84	3,48	2,737	40,5		
NC2C	71,4	5,80	0,329	0,321	8,23	3,69	3,33	75,4		
NC1-2C	24,90	2,025	0,2557	0,2350	2,100	2,315	2,096	16,57		
NC1F	141,9	11,54	0,2069	0,1887	9,61	1,784	1,651	74,4		
NRC	33,8	2,749	0,550	0,462	5,61	5,72	5,28	56,7		

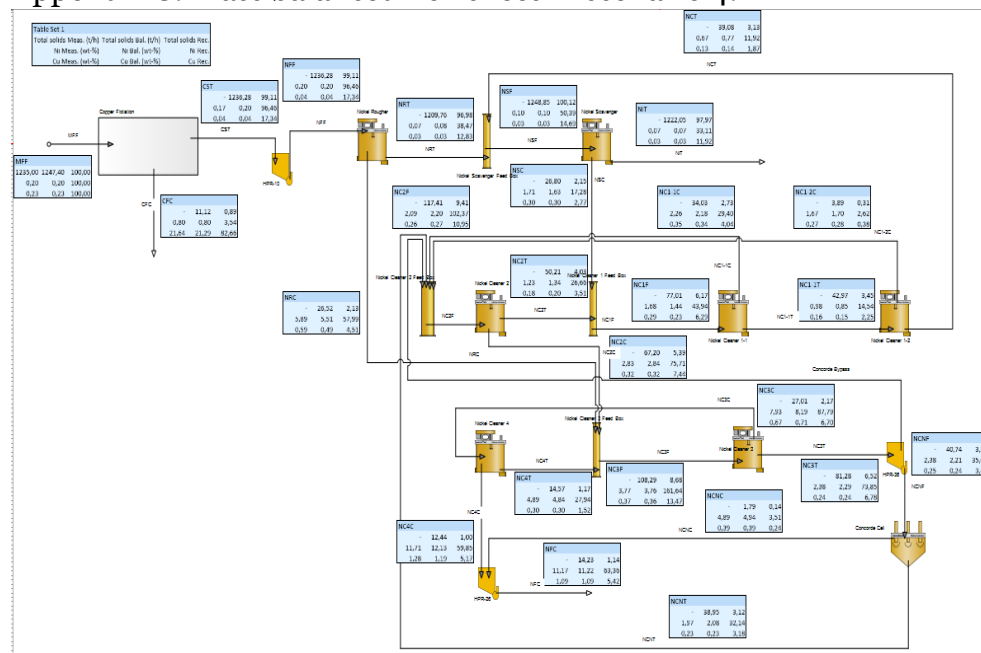
Appendix 6. Mass balanced flowsheet in scenario 3.



Appendix 7. Mass balanced results in scenario 4.

Stream	solids t/h	M solids t/hal	solids ReCu %	Meas. Cu % Bal.	Cu Rec %	Ni % Meas.	Ni % Bal.	Ni Rec %
NRT	1210	97,0	0,03123	0,03035	12,83	0,0682	0,0802	38,5
NFF	1236	99,1	0,0402	0,0402	17,34	0,1959	0,1967	96,5
NC2F	117,4	9,41	0,2596	0,2670	10,95	2,091	2,198	102,4
NSC	26,80	2,148	0,2982	0,2963	2,773	1,714	1,626	17,28
NC3F	108,3	8,68	0,368	0,356	13,47	3,77	3,76	161,6
NiT	1222	98,0	0,02797	0,02793	11,92	0,0681	0,0683	33,1
NC1-1T	43,0	3,45	0,1618	0,1497	2,247	0,980	0,853	14,54
NC1-1C	34,0	2,728	0,347	0,340	4,04	2,261	2,178	29,40
NC4C	12,44	0,997	1,282	1,190	5,17	11,71	12,13	59,8
NC4T	14,57	1,168	0,3024	0,2991	1,522	4,89	4,84	27,94
NC2T	50,2	4,03	0,1839	0,2004	3,51	1,234	1,339	26,66
NC2C	67,2	5,39	0,324	0,317	7,44	2,827	2,841	75,7
NCT	39,1	3,133	0,1251	0,1369	1,870	0,674	0,769	11,92
NSF	1249	100,1	0,0323	0,0337	14,69	0,1027	0,1017	50,4
NC1F	77,0	6,17	0,2925	0,2338	6,29	1,678	1,439	43,9
NC1-2C	3,89	0,3118	0,2749	0,2776	0,377	1,671	1,699	2,621
MFF	1247	100,0	0,2254	0,2295	100,0	0,2022	0,2021	100,0
NFC	14,23	1,141	1,091	1,090	5,42	11,17	11,22	63,4
NC3T	81,3	6,52	0,2362	0,2387	6,78	2,383	2,291	73,9
NCNF	40,7	3,27	0,2493	0,2404	3,42	2,379	2,206	35,7
NCNC	1,789	0,1434	0,390	0,390	0,2440	4,89	4,94	3,51
NC3C	27,01	2,165	0,670	0,710	6,70	7,93	8,19	87,8
NCNT	39,0	3,123	0,2257	0,2335	3,18	1,971	2,080	32,1
CST	1236	99,1	0,0369	0,0402	17,34	0,1669	0,1967	96,5
CFC	11,12	0,891	21,64	21,29	82,7	0,802	0,803	3,54
NRC	26,52	2,126	0,590	0,487	4,51	5,89	5,51	58,0
Concorde Bypass	40,5	3,25	0,2362	0,2370	3,36	2,383	2,376	38,2

Appendix 8. Mass balanced flowsheet in scenario 4.



Appendix 9. Mass balanced screening results in scenario 1.

Stream	Fraction	solids t/h	Re	Cu % Meas.	Cu % Bal.	Cu Rec %	Ni % Meas.	Ni % Bal.	Ni Rec %	Retained %t	Retained t	Retained
NFF	Bulk	1259	99,1	0,0410	0,0422	19,27	0,2213	0,1976	97,0			
NFF	-0,212 +0,106 mm	232,2	99,8	0,0581	0,0665	71,7	0,1097	0,0982	98,8	26,44	18,44	99,8
NFF	-0,106 +0,025 mm	487	98,5	0,03080	0,0323	13,54	0,2148	0,1935	95,1	35,8	38,7	98,5
NFF	-0,025 +0 mm	540	99,3	0,0400	0,0407	15,90	0,3123	0,2441	98,2	37,7	42,9	99,3
NFC	Bulk	16,78	1,320	1,143	1,130	6,87	10,16	8,71	57,0			
NFC	-0,212 +0,106 mm	1,755	0,754	1,800	1,822	14,84	5,34	5,03	38,2	10,45	10,46	0,754
NFC	-0,106 +0,025 mm	6,69	1,352	0,577	0,576	3,31	11,48	9,92	67,0	39,8	39,8	1,352
NFC	-0,025 +0 mm	8,34	1,533	1,335	1,428	8,62	9,52	8,50	52,8	49,7	49,7	1,533
NIT	Bulk	1242	97,7	0,02810	0,02752	12,40	0,0830	0,0827	40,1			
NIT	-0,212 +0,106 mm	230,5	99,0	0,0536	0,0532	56,8	0,0668	0,0606	60,6	16,39	18,55	99,0
NIT	-0,106 +0,025 mm	480	97,1	0,02640	0,02476	10,23	0,0606	0,0580	28,13	38,0	38,7	97,1
NIT	-0,025 +0 mm	532	97,8	0,01860	0,01890	7,28	0,1231	0,1146	45,4	45,6	42,8	97,8
MFF	Bulk	1258	1271	100,0	0,2170	100,0	0,2011	0,2017	100,0			
MFF	-0,212 +0,106 mm	232,8	100,0	0,1246	0,0926	100,0	0,0876	0,0991	100,0	16,80	18,31	100,0
MFF	-0,106 +0,025 mm	495	100,0	0,1860	0,2350	100,0	0,2351	0,2003	100,0	40,0	38,9	100,0
MFF	-0,025 +0 mm	544	100,0	0,3154	0,2539	100,0	0,323	0,2470	100,0	43,2	42,8	100,0
CFC	Bulk	11,99	0,943	18,66	18,58	80,7	0,640	0,634	2,964			
CFC	-0,212 +0,106 mm	0,571	0,2453	10,09	10,69	28,31	0,466	0,467	1,157	4,77	4,76	0,2453
CFC	-0,106 +0,025 mm	7,55	1,527	16,10	13,31	86,5	0,598	0,642	4,90	63,0	63,0	1,527
CFC	-0,025 +0 mm	3,86	0,710	24,21	30,05	84,1	0,619	0,643	1,849	32,2	32,2	0,710

Appendix 10. Scenario 2 screening mass balancing results.

Stream	Fraction	solids t/h	Re	Cu % Meas.	Cu % Bal.	Cu Rec %	Ni % Meas.	Ni % Bal.	Ni Rec %	Retained %t	Retained t	Retained
NFF	Bulk	1204	98,9	0,0431	0,0409	15,55	0,2223	0,2253	96,5			
NFF	-12 +0,106 mm	158,1	99,5	0,0620	0,0577	55,7	0,0789	0,0847	96,6	13,95	13,13	99,5
NFF	-0,06 +0,025 mm	464	98,8	0,0383	0,0330	16,85	0,1761	0,2041	95,5	38,0	38,5	98,8
NFF	-0,025 +0 mm	583	98,8	0,0497	0,0425	11,85	0,2691	0,2802	97,0	46,3	48,4	98,8
MFF	Bulk	1203	1218	100,0	0,2455	0,2598	100,0	0,2310	0,2309	100,0		
MFF	-12 +0,106 mm	158,8	100,0	0,0848	0,1030	100,0	0,1008	0,0872	100,0	11,07	13,04	100,0
MFF	-0,06 +0,025 mm	469	100,0	0,1616	0,1937	100,0	0,1870	0,2112	100,0	36,9	38,5	100,0
MFF	-0,025 +0 mm	590	100,0	0,3125	0,355	100,0	0,2671	0,2852	100,0	50,8	48,4	100,0
NFC	Bulk	15,19	1,247	1,073	1,087	5,22	11,13	11,34	61,2			
NFC	-12 +0,106 mm	0,625	0,394	2,594	2,590	9,90	5,84	5,95	26,88	4,11	4,12	0,394
NFC	-0,06 +0,025 mm	6,46	1,376	0,497	0,518	3,68	11,82	11,43	74,5	42,0	42,5	1,376
NFC	-0,025 +0 mm	8,11	1,375	1,266	1,425	5,52	9,86	11,67	56,3	52,6	53,4	1,375
NIT	Bulk	1189	97,6	0,02680	0,02750	10,33	0,0830	0,0833	35,2			
NIT	-12 +0,106 mm	157,5	99,2	0,0602	0,0476	45,8	0,0581	0,0614	69,8	14,57	13,24	99,2
NIT	-0,06 +0,025 mm	457	97,4	0,02940	0,02619	13,17	0,0454	0,0456	21,03	38,7	38,5	97,4
NIT	-0,025 +0 mm	574	97,4	0,02670	0,02302	6,32	0,1019	0,1194	40,8	45,5	48,3	97,4
CFC	Bulk	13,60	1,116	20,73	19,65	84,4	0,730	0,731	3,53			
CFC	-12 +0,106 mm	0,724	0,456	11,42	10,01	44,3	0,634	0,642	3,35	5,32	5,32	0,456
CFC	-0,06 +0,025 mm	5,54	1,180	15,86	13,65	83,1	0,759	0,806	4,50	40,2	40,7	1,180
CFC	-0,025 +0 mm	7,34	1,244	23,87	25,14	88,2	0,636	0,683	2,979	53,0	53,9	1,244

Appendix 11. Mass balancing results in scenario 3 screening.

Stream	Fraction	solids t/h	Re	Cu % Meas.	Cu % Bal.	Cu Rec %	Ni % Meas.	Ni % Bal.	Ni Rec %	Retained %t	Retained t	Retained
NFF	Bulk	1220	99,1	0,0421	0,0429	18,27	0,2552	0,2561	96,9			
NFF	-12 +0,106 mm	56,5	97,3	0,0651	0,0825	74,6	0,0771	0,0795	81,9	3,73	4,63	97,3
NFF	-0,06 +0,025 mm	475	99,1	0,0358	0,0403	20,26	0,2068	0,2191	96,2	36,4	38,9	99,1
NFF	-0,025 +0 mm	689	99,2	0,0373	0,0414	15,36	0,322	0,2961	97,7	53,1	56,5	99,2
MFF	Bulk	1218	1231	100,0	0,2282	0,2327	100,0	0,2619	0,2618	100,0		
MFF	-12 +0,106 mm	58,1	100,0	0,0865	0,1075	100,0	0,0712	0,0944	100,0	4,99	4,72	100,0
MFF	-0,06 +0,025 mm	479	100,0	0,1849	0,1973	100,0	0,2072	0,2257	100,0	33,9	38,9	100,0
MFF	-0,025 +0 mm	694	100,0	0,3115	0,2676	100,0	0,329	0,3007	100,0	54,0	56,4	100,0
NFC	Bulk	19,36	1,573	0,891	0,884	5,98	10,72	10,78	64,7			
NFC	-12 +0,106 mm	2,863	4,93	2,261	0,844	38,7	3,20	0,754	39,3	15,03	14,79	4,93
NFC	-0,06 +0,025 mm	7,28	1,520	0,478	0,505	3,89	10,56	11,46	77,2	38,0	37,6	1,520
NFC	-0,025 +0 mm	9,21	1,328	1,006	1,196	5,94	10,17	13,35	58,9	48,1	47,6	1,328
NIT	Bulk	1200	97,5	0,02980	0,02933	12,29	0,0862	0,0864	32,2			
NIT	-12 +0,106 mm	53,7	92,3	0,0547	0,0418	35,9	0,0606	0,0435	42,6	14,91	4,47	92,3
NIT	-0,06 +0,025 mm	467	97,6	0,02420	0,0331	16,37	0,0460	0,0439	18,99	37,7	38,9	97,6
NIT	-0,025 +0 mm	679	97,9	0,01780	0,02576	9,43	0,1178	0,1190	38,8	46,0	56,6	97,9
CFC	Bulk	11,09	0,901	21,45	21,11	81,7	0,891	0,891	3,066			
CFC	-12 +0,106 mm	1,584	2,726	12,25	1,000	25,36	0,662	0,626	18,09	14,09	14,29	2,726
CFC	-0,06 +0,025 mm	4,26	0,890	17,40	17,68	79,7	0,872	0,960	3,79	37,2	38,4	0,890
CFC	-0,025 +0 mm	5,24	0,756	24,77	29,98	84,6	0,815	0,915	2,298	45,4	47,3	0,756

Appendix 12. Mass balancing results in scenario 4 screening.

Stream	Fraction	solids t/h	Re	Cu % Meas.	Cu % Bal.	Cu Rec %	Ni % Meas.	Ni % Bal.	Ni Rec %	Retained %t	Retained %t	Retained %t
NFF	Bulk	1236	99,2	0,0377	0,0385	18,19	0,1975	0,1942	97,2		100,0	99,2
NFF	12 +0,106 mm	175,6	99,8	0,0572	0,0615	70,0	0,0572	0,0655	98,3	14,08	14,20	99,8
NFF	06 +0,025 mm	484	99,3	0,03120	0,0347	21,09	0,1676	0,1845	97,3	38,3	39,1	99,3
NFF	0,025 +0 mm	577	99,0	0,0342	0,0347	12,01	0,2645	0,2416	97,1	46,1	46,7	99,0
NIT	Bulk	1222	98,1	0,02860	0,02829	13,20	0,0675	0,0675	33,4		100,0	98,1
NIT	12 +0,106 mm	174,8	99,4	0,0564	0,0519	58,9	0,0484	0,0457	68,4	16,10	14,31	99,4
NIT	06 +0,025 mm	477	98,0	0,02530	0,02820	16,88	0,0401	0,0374	19,45	38,0	39,1	98,0
NIT	0,025 +0 mm	570	97,7	0,01820	0,02112	7,22	0,0987	0,0993	39,4	44,9	46,6	97,7
MFF	Bulk	1235	100,0	0,2193	0,2102	100,0	0,1982	0,1983	100,0		100,0	100,0
MFF	12 +0,106 mm	175,9	100,0	0,0723	0,0876	100,0	0,0755	0,0665	100,0	12,85	14,12	100,0
MFF	06 +0,025 mm	487	100,0	0,1801	0,1636	100,0	0,1704	0,1883	100,0	39,2	39,1	100,0
MFF	0,025 +0 mm	583	100,0	0,2986	0,2860	100,0	0,2714	0,2465	100,0	46,5	46,8	100,0
NFC	Bulk	14,69	1,179	0,892	0,888	4,99	11,01	10,74	63,8		100,0	1,179
NFC	12 +0,106 mm	0,712	0,405	2,522	2,413	11,14	5,00	4,92	29,95	4,83	4,84	0,405
NFC	06 +0,025 mm	6,59	1,352	0,521	0,509	4,21	12,25	10,84	77,9	43,8	44,8	1,352
NFC	0,025 +0 mm	7,39	1,269	1,084	1,080	4,79	9,67	11,20	57,7	49,0	50,3	1,269
CFC	Bulk	9,45	0,759	21,97	22,66	81,8	0,731	0,730	2,794		100,0	0,759
CFC	12 +0,106 mm	0,354	0,2010	14,25	13,07	29,98	0,556	0,560	1,692	3,74	3,74	0,2010
CFC	06 +0,025 mm	3,37	0,691	17,49	18,68	78,9	0,694	0,733	2,691	35,1	35,6	0,691
CFC	0,025 +0 mm	5,73	0,983	24,37	25,59	88,0	0,672	0,739	2,949	59,3	60,6	0,983

Appendix 13. Mass balancing results in scenario 1 screening of the Concorde Cell™.

Stream	Fraction	solids t/h	Re	Cu % Meas.	Cu % Bal.	Cu Rec %	Ni % Meas.	Ni % Bal.	Ni Rec %	Retained %t	Retained %t	Retained %t
NCNF	Bulk	100,0	100,0	0,481	0,478	100,0	4,34	4,40	100,0		100,0	100,0
NCNF	212 +0,106 mm	3,4	100,0	1,661	1,693	100,0	0,77	0,80	100,0	1,4	3,4	100,0
NCNF	106 +0,025 mm	23,19	100,0	0,517	0,502	100,0	5,81	6,61	100,0	18,99	23,19	100,0
NCNF	0,025 +0 mm	73,400	100,0	0,429	0,414	100,0	3,390	3,860	100,0	79,600	73,400	100,0
NCNT	Bulk	71,0	71,0	0,2674	0,2682	39,8	2,196	2,134	34,5		100,0	71,0
NCNT	212 +0,106 mm	2,2	65,2	1,4180	1,3900	53,5	0,427	0,421	34,3	1,5	3,1	65,2
NCNT	106 +0,025 mm	12,36	53,3	0,401	0,400	42,4	3,072	3,024	24,40	17,34	17,42	53,3
NCNT	0,025 +0 mm	56,400	76,8	0,199	0,195	36,2	1,996	2,007	39,90	76,900	79,500	76,8
NCNC	Bulk	29,02	29,01	0,988	0,992	60,2	10,47	9,93	65,5		100,0	29,01
NCNC	212 +0,106 mm	1,19	34,80	2,292	2,261	46,5	1,56	1,51	65,7	4,0	4,1	34,80
NCNC	106 +0,025 mm	10,82	46,7	0,617	0,620	57,6	11,16	10,71	75,6	37,9	37,3	46,7
NCNC	0,025 +0 mm	17,010	23,2	1,151	1,140	63,8	9,820	10,030	60,1	53,40	58,60	23,2

Appendix 14. Mass balancing results of scenario 4 screening of the Concorde Cell™.

Stream	Fraction	solids t/h	Re	Cu % Meas.	Cu % Bal.	Cu Rec %	Ni % Meas.	Ni % Bal.	Ni Rec %	Retained %t	Retained %t	Retained %t
NCNF	Bulk	100,0	100,0	0,246	0,246	100,0	2,47	2,47	100,0		100,0	100,0
NCNF	212 +0,106 mm	2,0	100,0	1,509	1,373	100,0	0,69	0,69	100,0	1,2	2,0	100,0
NCNF	106 +0,025 mm	27,53	100,0	0,356	0,352	100,0	1,19	1,16	100,0	26,80	27,53	100,0
NCNF	0,025 +0 mm	70,400	100,0	0,172	0,172	100,0	2,780	3,034	100,0	70,400	70,400	100,0
NCNT	Bulk	82,7	82,7	0,2256	0,2256	76,0	2,013	2,012	67,4		100,0	82,7
NCNT	212 +0,106 mm	1,6	79,2	1,2090	1,2750	73,6	0,646	0,644	74,0	1,0	1,9	79,2
NCNT	106 +0,025 mm	21,15	76,8	0,353	0,351	76,6	0,701	0,718	47,40	24,52	25,56	76,8
NCNT	0,025 +0 mm	60,000	85,2	0,156	0,153	76,1	2,348	2,505	70,30	72,500	72,500	85,2
NCNC	Bulk	17,26	17,26	0,342	0,341	24,0	4,68	4,67	32,6		100,0	17,26
NCNC	212 +0,106 mm	0,42	20,79	1,736	1,746	26,4	0,86	0,86	26,0	1,7	2,4	20,79
NCNC	106 +0,025 mm	6,38	23,2	0,373	0,355	23,4	2,55	2,64	52,6	36,3	37,0	23,2
NCNC	0,025 +0 mm	10,450	14,8	0,297	0,277	23,9	5,730	6,070	29,7	60,50	60,60	14,8